

Learning Interpretable Models Using Uncertainty Oracles

Abhishek Ghose, Balaraman Ravindran

¹Indian Institute of Technology, Madras
abhishek.ghose.82@gmail.com

Abstract

A desirable property of interpretable models is small size, so that they are easily understandable by humans. This leads to the following challenges: (a) small sizes typically imply diminished accuracy, and (b) bespoke levers provided by model families to restrict size, e.g., L1 regularization, might be insufficient to reach the desired size-accuracy trade-off.

We address these challenges here. Earlier work has shown that learning the training distribution creates accurate small models. Our contribution is a new technique that exploits this idea. The training distribution is encoded as a Dirichlet Process to allow for a flexible number of modes that is learnable from the data. Its parameters are learned using Bayesian Optimization; a design choice that makes the technique applicable to non-differentiable loss functions. To avoid the challenges with high dimensionality, the data is first projected down to one-dimension using uncertainty scores of a separate probabilistic model, that we refer to as the uncertainty oracle.

We show that this technique addresses the above challenges: (a) it arrests the reduction in accuracy that comes from shrinking a model (in some cases we observe $\sim 100\%$ improvement over baselines), and also, (b) that this may be applied with no change across model families with different notions of size; results are shown for Decision Trees, Linear Probability models and Gradient Boosted Models.

Additionally, we show that (1) it is more accurate than its predecessor, (2) requires only one hyperparameter to be set in practice, (3) accommodates a multi-variate notion of model size, e.g., both maximum depth of a tree and number of trees in Gradient Boosted Models, and (4) works across different feature spaces between the uncertainty oracle and the interpretable model, e.g., a Gated Recurrent Unit trained using character sequences may be used as an oracle for a Decision Tree that ingests character n-grams as features.

1 Introduction

In recent years, Machine Learning (ML) models have become increasingly pervasive in various real world systems. This has led to a growing emphasis on models to be *understandable*, especially in domains where the cost of being wrong is prohibitively high, e.g., medicine and healthcare (Caruana et al. 2015; Ustun and Rudin 2016; Tjoa and Guan 2021; J. Wang et al. 2022), defence applications (Gunning 2016; Moustafa et al. 2023), law enforcement (Angwin et al. 2016; Larson et al. 2016; Herrewijn et al. 2024).

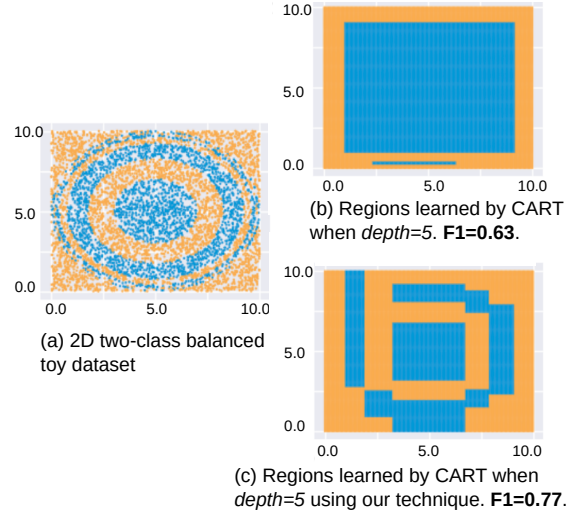


Figure 1: Application of our technique is shown on the toy dataset in (a). Learning a DT constrained to a depth of 5 using the CART algorithm produces the regions shown in (b). Additionally learning the training distribution using our technique produces the regions in (c). For both (b) and (c) the F1-macro scores on a held-out set are reported.

An important aspect of model interpretability is its size (smaller is better); this is both shown in various user studies (Feldman 2000; Kulesza et al. 2013; Piltaver et al. 2016; Lage et al. 2019; Poursabzi-Sangdeh et al. 2021), and is evidenced by its popularity as an algorithm design criteria (Tibshirani 1996; Ribeiro, Singh, and Guestrin 2016; Herman 2017; Lipton 2018; Murdoch et al. 2019; Lakkaraju, Bach, and Leskovec 2016; Good et al. 2023). However, small size typically implies high bias and thus, relatively lower accuracy. A practitioner may control this size-accuracy trade-off using bespoke levers offered by a training algorithm, e.g., early stopping in Decision Trees (DT), L1 regularization in linear models. This doesn't entirely and conveniently solve the trade-off problem since (1) to get to the desired trade-off, one may need to be intimately aware of how various hyperparameters (hence referred to as *hyperparams*) interact, and (2) the desired trade-off might not even be possible for a

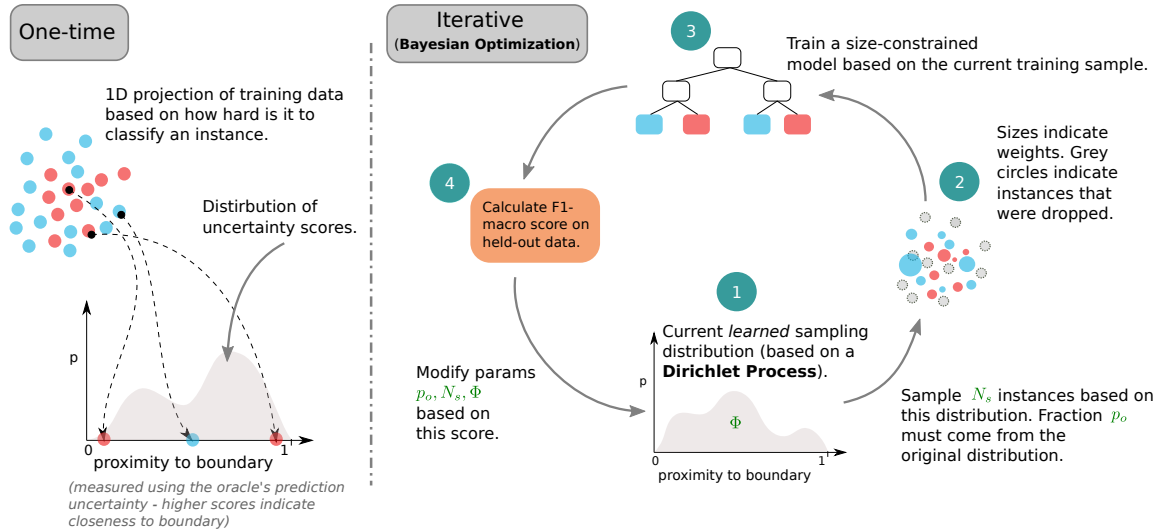


Figure 2: Overview of our technique. *Left*: Training instances are characterized by their proximity to class boundaries. As a proxy for this quantity, we use the prediction uncertainty scores of a probabilistic oracle (these may also be seen as an 1D *projection*): higher uncertainty indicates proximity to a boundary. These scores are calculated *once*. *Right*: The size-constrained model is learned iteratively. A sampling distribution, parameterized by Φ , over the uncertainty values (shown in Step 1) is used to sample training instances (as in Step 2), which is used to train a size-constrained model (shown in Step 3). Its accuracy on a held-out set - Step 4 - is used to modify Φ . This loop, Steps 1-4, is executed by a BayesOpt algorithm.

model family within its hyperparameter search space.

Here we propose a model-agnostic¹ technique that is shown to often produce better accuracies for small-sized models on classification problems. The underlying strategy is to learn a distribution over training instances and accordingly create a new training set; this has been shown to produce small accurate models (Ghose and Ravindran 2020). Since a training distribution maybe learned for any setting of a model’s hyperparams, the technique maybe seen as a “meta” algorithm, where the size constraint is enforced using standard hyperparams, and then accuracy is further improved by learning a distribution over training data.

We show its application on the toy dataset in Figure 1(a). Figure 1(b) visualizes class regions learned by a DT of $depth = 5$ using the CART (Breiman et al. 1984) algorithm. The F1-macro score on a held-out set is 0.63. When the training distribution is also learned using our technique, we obtain the regions in Figure 1(c) and a F1-macro score of 0.77.

The workings of the technique itself are presented at a high-level in Figure 2. Instead of learning the training distribution directly, which might be expensive because of the dimensionality of the data, we first project the data down to one dimension. This is done just once, and is shown in the left panel in Figure 2. Since we are solving for classification, we pick this dimension to be a numeric indicator of how close an instance is to a class boundary. As a convenient proxy, we train a separate highly accurate probabilistic

oracle model on the training data², and use its prediction *uncertainty* score as the projected value; higher uncertainty scores ideally denote greater proximity to class boundaries.

The distribution is modeled as an *Infinite Beta Mixture Model* using a *Dirichlet Process*, which is *iteratively* learned. Step 1 on the right panel in Figure 2 shows the current distribution, based on which training data is sampled (Step 2). The size-constrained model of interest is then trained on this sample - Step 3 - and its accuracy on a held-out set is calculated - Step 4. This score is used as a feedback for the optimizer which repeats the process to learn better distribution parameters. We use *Bayesian Optimization (BayesOpt)* (Shahriari et al. 2016; Garnett 2023) to accommodate models with non-differentiable losses.

□

Our contributions in this work are: we propose a technique that (a) produces small accurate models by learning a training distribution. It is shown to provide relative improvements of $\sim 100\%$ in some cases. (b) is model-agnostic, where the models may also have non-differentiable losses, e.g., DTs. Additionally, we show that: (1) it is more accurate than its predecessor (Ghose and Ravindran 2020), (2) is practically convenient since only one hyperparameter needs to be set, (3) allows for model sizes to be defined by more than one component, e.g., number of trees and depth per tree in Gradient Boosted Models (GBM) (Friedman 2001), and (4) can use oracles trained on a different feature representation of the same data. The last property is useful since it allows for a broad choice of oracles. We show an example of this later.

¹We use the term to mean agnostic to the model *family*, as is accepted usage in the area of XAI, e.g., SHAP (Lundberg and Lee 2017), LIME (Ribeiro, Singh, and Guestrin 2016) are considered to be model-agnostic.

²In Figure 1, the oracle used is a Gradient Boosted Model.

The rest of the paper is organized as follows: we first review related work in §2. We then detail our technique in §3. We follow that up with rigorous empirical validations in §4.1 and comparisons to prior work in §4.2. After discussing additional applications, in §5 and §6, we conclude the paper with a summary and notes on future work in §7.

2 Related Work

The concept of using a different training distribution relative to test is common in the case of class imbalance, e.g., undersample the majority class data (Japkowicz and Stephen 2002; Chawla et al. 2002; He et al. 2008; Santhiappan, Chelladurai, and Ravindran 2018), but it was shown to be a general strategy for improving accuracy in Ghose and Ravindran (2020). Their technique relies on a specialized DT called *density trees*, that encodes the geometric placement of training data, and facilitates learning a distribution. In our view, notwithstanding its interesting properties, the accuracy of density trees implicitly limit the effectiveness of their technique. This work may be seen as a non-trivial extension: a model (the uncertainty oracle) from an arbitrary model family may be used, resulting in greater flexibility and accuracy.

The interaction of two models - the oracle and the interpretable model - might suggest an overlap with the area of *Knowledge Distillation* (Gou et al. 2021). But there is a critical difference: *in theory, we don't require the oracle model*; its sole purpose here is to reduce computational cost. Its a dimensionality reduction tool³ that is invoked once outside the main learning loop (see Figure 2). This peripheral role is emphasized by the fact that the labels predicted by the oracle are ignored.

For similar reasons, this technique must not be seen as a successor to model explanation techniques where we seek to explain the oracle, e.g., Craven and Shavlik (1995); Alaa and van der Schaar (2019); again, the key difference is that any form of alignment/fidelity wrt the oracle is ignored.

Since Ghose and Ravindran (2020) represents the work closest to ours, we benchmark our technique against their approach.

3 Methodology

We describe our technique in detail in this section. But first, we introduce some notation.

3.1 Terminology and Notation

1. A dataset is denoted as a set of instance-label pairs, $D = \{(x_1, y_1), (x_2, y_2), \dots, (x_N, y_N)\}$. A joint distribution over a dataset is denoted by $p(X, Y)$.
2. To distinguish between the distribution we are given (in form of the dataset) and the one we learn, we refer to the former as the *original* distribution. In *all* experiments here, the test and held-out data follow the original distribution; for the training data, we learn a new distribution.

³There are others possible, e.g., given point A , use the number of points of different classes among its nearest neighbors to estimate A 's proximity to a class boundary.

3. We let $acc(M, p)$ denote the classification accuracy of model M on data represented by the joint distribution $p(X, Y)$. Here acc is a generic metric, and may be implemented as *AUC*, *F1-macro* score, etc.
4. $train_{\mathcal{F}, f}(p, \eta)$ is understood to produce a model of size η (for some pre-decided notion of size) from the model family \mathcal{F} using a specific training algorithm f .

For instance, \mathcal{F} might represent DTs and f might be the CART algorithm, and $\eta = 5$ might denote a DT of *depth* = 5. We let $\eta = *$ denote unbounded size.

Let us state our objective using this notation. Typically, a model is trained on the same distribution as the test (on which it is evaluated), i.e., we evaluate $acc(train_{\mathcal{F}, f}(p, \eta), p)$. Here, the training distribution is allowed to be different relative to the test. In other words, we seek p' s.t.:

$$\arg \max_{p'} acc(train_{\mathcal{F}, f}(p', \eta), p) \quad (1)$$

3.2 Algorithm

Referring to the high-level flow in Figure 2, we note that the proposed technique relies on a few important ingredients. These are discussed below:

1. **Uncertainty score:** This is needed for the one-time projection using the oracle. There are multiple ways to measure prediction uncertainty; here we choose *margin uncertainty* (Scheffer, Decomain, and Wrobel 2001), since (a) it accounts for prediction probabilities of different classes, (b) while also producing high scores even with two dominant predicted classes in a setting that has more classes. The uncertainty score for x , as provided by model M , is denoted by $u_M(x) \in [0, 1]$. The margin uncertainty is calculated as:

$$u_M(x) \leftarrow 1 - (p_{C_1} - p_{C_2}) \quad (2)$$

Here, p_{C_1} and p_{C_2} denote the probabilities of the most confident and next most confident classes. See §A.1 for further details.

2. **Density model:** Since we want to *learn* a distribution, we want the representation to be flexible. We encode the density as a *mixture model* of *Beta* distributions. We use the latter since their support matches the range of uncertainty scores, i.e., $u_M(x) \in [0, 1]$. We also note that a *Beta* mixture model can approximate any distribution in $[0, 1]$ arbitrarily well given a sufficient number of components (Diaconis and Ylvisaker 1983). Further, in the interest of flexibility, we refrain from explicitly dictating the number of *Beta* components, and thus, we use an *Infinite Beta Mixture Model (IBMM)*, where the component assignments are decided by a standard *Dirichlet Process (DP)* (Ferguson 1973). Another advantage of this formulation is that it leads to a fixed number of parameters irrespective of the number of active components⁴, which

⁴Contrast this with a *Gaussian Mixture Model (GMM)* where the number of parameters change with the number of components. GMMs have a *conditional* parameter space, and most optimizers handle fixed parameter spaces.

makes it easy to pick an optimizer. We note here that Ghose and Ravindran (2020) also use a DP-based IBMM, but for modeling the height of density trees.

Two sets of parameters are required to describe this density model:

- (a) The shape parameters A_i, B_i of the i^{th} *Beta* component. These are separately sampled from prior distributions that are themselves *Beta* distributions, with shape parameters a, b and a', b' respectively. Since naively doing this would restrict A_i or B_i to *Beta*'s support, i.e., $[0, 1]$, we also multiply the sampled value by a variable *scale*, that we set to be large enough to cover the family of component distributions we require⁵. Effectively then, $A_i \sim scale \times Beta(a, b)$ and $B_i \sim scale \times Beta(a', b')$.
- (b) The DP needs just a *concentration* parameter $\alpha \in \mathbb{R}_{>0}$ that decides the number of active components, i.e., ones with instances assigned to them⁶.

In all, the density model requires *five* parameters, which we denote as $\Psi = \{\alpha, a, b, a', b'\}$. To sample N_s instances given Ψ , we first determine the number of instances per component using a standard technique like the *Chinese Restaurant Process* (Aldous 1985) and then sample component-wise. Please see §A.2 for details.

3. **Optimization:** As mentioned earlier, we use BayesOpt to accommodate non-differentiable losses. Its resilience to noise is also beneficial since observed model accuracies may be noisy, due to randomized initialization of model parameters, different dataset splits across trials, etc. Specifically, we use the *hyperopt* library (Bergstra, Yamins, and Cox 2013), which implements the *Tree Structured Parzen Estimator (TPE)* algorithm (Bergstra et al. 2011).

For optimization, in addition to Ψ , we retain the following parameters originally introduced in Ghose and Ravindran (2020):

- (a) N_s : This is the sample size - this is also learned.
- (b) $p_o \in [0, 1]$: Proportion of the new training sample that is constituted by a uniform sample from the original training data. This serves two purposes: (1) it acts as a “shortcut” for the optimizer to mix in the original distribution as needed, and (2) it serves as a “probe variable”, i.e., it shows how much of the original distribution is actually needed for good accuracies.

Accounting for these, we now have a total of *seven* optimization variables: $\Psi = \{\alpha, a, b, a', b'\}, p_o, N_s$, which are iteratively optimized, till the budgeted number of iterations, T , are exhausted. These variables are collectively denoted as $\Phi = \{\Psi, N_s, p_o\}$. Algorithm 1 outlines the overall technique; here the interpretable and oracle model families are denoted by \mathcal{I} and \mathcal{O} , and the respective training algorithms are denoted by h and g respectively. §A.4

⁵**NOTE:** This is fixed at a value of 10000 and not learned; hence it isn't counted as a parameter.

⁶Of course, in theory, there are an infinite number of components, and the number of active components grows with data.

Algorithm 1: Learning interpretable model using oracle

Data: Dataset D , model size η , $train_{\mathcal{O},h}()$, $train_{\mathcal{I},g}()$, iterations T
Result: Optimal parameters Φ^* , test set accuracy s_{test} at Φ^* , and interpretable model M^* at Φ^*

- 1 Create splits $D_{train}, D_{val}, D_{test}$ from D , stratified wrt labels. Here $|D_{train}| : |D_{val}| : |D_{test}| :: 60 : 20 : 20$.
- 2 $M_O \leftarrow train_{\mathcal{O},h}(D_{train}, *)$
- 3 **for** $t \leftarrow 1$ **to** T **do**
- 4 $\Phi_t \leftarrow suggest(s_0, s_1, \dots, s_{t-1}, \Phi_0, \Phi_1, \dots, \Phi_{t-1})$
 // s_0, Φ_0 initialized at $t = 0$, see text. Note:
 $\Phi_t = \{\Psi_t, N_{s,t}, p_{o,t}\}$ where
 $\Psi_t = \{\alpha_t, a_t, b_t, a'_t, b'_t\}$.
- 5 $N_o \leftarrow p_{o,t} \times N_{s,t}$
- 6 $N_u \leftarrow N_{s,t} - N_o$
- 7 $D_o \leftarrow$ uniformly sample with replacement N_o points from D_{train}
- 8 $D_u \leftarrow$ sample N_u points from D_{train} using the DP-based IBMM given current values for $N_u, M_O, D_{train}, \Psi_t$ // see Algorithm A.2 for details
- 9 $D_s \leftarrow D_o \uplus D_u$ // D_o, D_u are assumed to be multisets
- 10 $M_t \leftarrow train_{\mathcal{I},g}(D_s, \eta)$
- 11 $s_t \leftarrow acc(M_t, D_{val})$
- 12 **end**
- 13 $t^* \leftarrow \arg \max_t \{s_1, s_2, \dots, s_{T-1}, s_T\}$
- 14 $\Phi^* \leftarrow \Phi_{t^*}$
- 15 $M^* \leftarrow M_{t^*}$
- 16 $s_{test} \leftarrow acc(M^*, D_{test})$
- 17 **return** Φ^*, s_{test}, M^*

provides additional details around model selection, robust estimation of *acc*, etc.

Optimization variables and parameters: The task of the optimizer is to find Φ that maximizes the held-out accuracy (line 11 in Algorithm 1) within T iterations. The optimizer here accepts *box constraints*, and as such their lower/upper bounds, which need to be set by the user, are *parameters* (along with T) of the technique. We discuss in §A.3 that reasonable defaults exist for parameters Φ , e.g., its easy to see $p_o \in [0, 1]$. So, in practice T is the only parameter that a user needs to determine.

Smoothing: A final practical consideration is the smoothness of the optimization landscape. Uncertainty scores over the training data may often result in a density that isn't smooth, making it difficult for the optimizer to identify a good maxima. We redress this by explicitly smoothing the density. We detail this in §A.5.

This concludes our discussion of algorithmic details; next, we look at empirical validation.

4 Experiments

This section covers the various empirical investigations. Some common elements across our experiments are:

1. **Datasets:** We use the following 13 publicly available datasets for our experiments: *cod-rna*, *ijcnn1*, *higgs*, *cov-type.binary*, *phishing*, *ala*, *pendigits*, *letter*, *Sensorless*, *senseit_aco*, *senseit_sei*, *covtype*, *connect-4*. These were obtained from the LIBSVM website (Chang and Lin 2011). For details, such as number of classes and extent of imbalance, please see §A.7.

10000 instances from each dataset are used. The split ratio used in Algorithm 1 is $|D_{train}| : |D_{val}| : |D_{test}| :: 60 : 20 : 20$, where the splits are stratified wrt labels.

2. **Interpretable model families:** we use *Linear Probability Models (LPM)*⁷ and the DTs (produced by the CART algorithm). The notion of model size for LPMs is the number of non-zero coefficients, and sizes $\eta \in \{1, 2, \dots, 15\}$ are explored (except for *cod-rna*, that has 8 features, and so we cannot have a sizes greater than 8).

For DTs, the notion of size is depth. For a dataset, we first learn a tree (with no size constraints) with the highest *F1-macro* score using standard 5-fold cross-validation. We refer to this as the optimal tree T_{opt} , and its depth as $depth(T_{opt})$. We then explore model sizes $\eta \in \{1, 2, \dots, \min(depth(T_{opt}), 15)\}$. Stopping early makes sense since the model is saturated in its learning at $depth(T_{opt})$; changing the input distribution is not helpful beyond this point.

3. **Oracle families:** As oracles we use *Random Forests (RF)* (Breiman 2001) and *GBMs* (Friedman 2001). Both oracles were calibrated (Platt 1999; Niculescu-Mizil and Caruana 2005) for reliable probability estimates.
4. **Optimization budget:** For DTs, we use $T = 3000$, while for LPMs $T = 1000$ is used. These values were determined based on limited search. The budget for LPMs is lower since for multi-class datasets (7 of 13 here) we construct one-vs-all models which makes training LPMs time-consuming.

Our implementation primarily utilizes the following libraries: *scikit-learn* (Pedregosa et al. 2011), *scipy* (Jones et al. 2001), *LightGBM* (Ke et al. 2017).

First, we look at the validation results.

4.1 Validation

In these experiments, our goal is to scrutinize how our technique performs. For various combinations of models and oracles, i.e., $\{LPM, DT\} \times \{GBM, RF\}$, we measure the percentage relative improvement in the *F1-macro* score (on D_{test}) in terms of the baseline score $F1_{test}^{base}$ and the one produced by our model, $F1_{test}^*$:

$$\delta F1_{test} = \frac{100 \times (F1_{test}^* - F1_{test}^{base})}{F1_{test}^{base}} \quad (3)$$

⁷We have not used the more common *Logistic Regression* because: (1) LPMs are considered more interpretable (Mood 2010), and (2) LPMs results are indicative of behavior of linear models in general.

We use the macro score since its not impacted by class imbalance.

In the interest of robustness we run *five trials* per configuration, i.e., a combination of dataset, oracle family, model family and size, and utilize the validation set to accept the model produced by our technique M^* . Specifically: indexing trials with i , we conduct an independent *t-test* on $\{F1_{val}^*\}_{1 \leq i \leq 5}$ and $\{F1_{val}^{base}\}_{1 \leq i \leq 5}$. The null hypothesis is that M^* doesn't produce results different M^{base} . If we can reject the null at a significance of $p = 0.1$, we report $\delta F1_{test}$ as in Equation 3⁸, else we report $\delta F1_{test} = 0$, i.e., we reject M^* . Here $\delta F1_{test} \in (-\infty, \infty)$; negative values are possible since we pick a model based on D_{val} while we report based on D_{test} .

Table 1 shows a portion of the results in the interest of space - for complete results (and analysis of statistical significance), please see §A.8.

Observations: We highlight some interesting trends:

1. We note that the incidence of negative improvements if fairly low. Of course, this result set is incomplete, but referring to the complete set in §A.8, we note that only 13 of 690 non-null observations, or 1.88%, are negative. The average negative improvement is -0.24% .
2. As model size increases (left to right in Table 1), positive improvements (which can be high for small sizes, e.g., $> 100\%$) tend to reduce. This makes intuitive sense since beyond a certain model size, when all informative patterns in the data have been captured, modifying the training distribution should not have much/any effect.
3. For DTs, the drop in improvements happen earlier than for LPMs. An intuitive explanation for this is that an unit increase in size for the LPM and DT do not lead to identical increase in capacity. DTs are non-linear models to begin with, and then, increasing their depth by one leads to a much larger increment in capacity, e.g., it doubles the number of leaves for a binary tree.

Points #2 and #3 above are similar to trends reported in Ghose and Ravindran (2020), and thus they informally validate that these techniques are at least qualitatively similar.

4.2 Comparison to Previous Work

In this section, we compare our technique to the one based on density trees. Please see §2 for why we consider this to be the incumbent.

Their metric is slightly different from ours. Instead of reporting results for $F1^*$, they report them for $\max(F1^*, F1^{base})$. This is an "outcome-centric" view⁹, where you can't do worse than your best model. For this case, $\delta F1_{test} \in [0, \infty)$. We also follow this scoring scheme in this section to match their reporting.

We report two scores for comparison:

⁸The test scores from different trials are averaged first.

⁹Another reason provided is that with a sufficient budget the optimizer will eventually learn to set $p_o = 1$, thus emulating M^{base} exactly, if M^{base} is indeed the best possible model. In this case $\delta F1 = 0$ as per Equation 3.

Table 1: This table shows the average improvements, $\delta F1$, over **five runs** for the combinations **model**= $\{LPM, DT\}$ and **oracle**= GBM . The improvements are measured relative to the model at the first iteration. Here, $\delta F1 \in (-\infty, \infty)$. Negative improvements are shown in underlined. **Complete results, including analysis of statistical significance, are presented in §A.8.**

dataset	model_ora	1	2	3	4	5	6	7	8	9	10	11	12	13	14	15
cod-rna	lpm_gbm	1.39	12.53	14.76	15.73	14.97	12.00	0.00	0.08	-	-	-	-	-	-	-
	dt_gbm	0.00	0.00	0.00	1.26	0.00	0.00	0.00	0.00	<u>-0.28</u>	0.08	-	-	-	-	-
ijcnn1	lpm_gbm	<u>-0.16</u>	3.36	3.93	0.00	5.19	4.18	3.85	3.79	3.69	2.99	2.97	3.21	3.11	3.26	3.02
	dt_gbm	1.96	12.00	10.15	11.37	10.63	7.18	3.63	4.52	2.91	1.78	1.93	2.29	1.47	2.26	0.00
higgs	lpm_gbm	29.29	17.80	11.40	6.56	3.06	2.68	3.16	2.90	2.67	2.82	2.65	1.79	2.62	2.19	1.63
	dt_gbm	0.00	0.00	1.86	0.26	0.93	0.45	-	-	-	-	-	-	-	-	-
covtype.binary	lpm_gbm	76.52	66.39	29.17	12.51	9.18	5.28	4.94	4.56	3.92	3.56	3.62	3.31	2.59	2.83	2.39
	dt_gbm	0.00	0.00	2.35	1.27	1.18	1.11	0.00	0.00	0.00	-	-	-	-	-	-
phishing	lpm_gbm	0.00	1.88	2.88	3.05	3.22	3.25	2.99	1.69	1.42	1.45	1.29	0.00	0.00	0.00	0.00
	dt_gbm	0.00	0.00	0.00	0.07	0.39	0.00	0.28	0.22	0.44	0.23	0.00	0.00	0.00	0.00	0.00
a1a	lpm_gbm	0.00	2.55	7.58	8.98	8.40	8.03	8.90	8.23	8.17	7.90	5.96	7.10	6.97	6.18	5.73
	dt_gbm	0.00	5.54	2.39	3.84	3.55	2.55	1.51	2.25	4.87	-	-	-	-	-	-
pendigits	lpm_gbm	51.39	23.44	16.18	8.95	8.84	6.63	4.86	1.83	2.27	2.16	2.44	2.16	3.33	2.97	2.73
	dt_gbm	14.02	6.72	5.11	13.14	6.42	4.20	2.46	1.09	0.98	0.16	<u>-0.26</u>	0.00	0.00	0.00	0.00
letter	lpm_gbm	57.06	48.48	59.85	29.76	36.09	19.27	20.37	16.08	17.55	15.16	17.26	16.51	18.46	17.19	15.55
	dt_gbm	0.00	13.98	25.05	33.96	32.05	15.49	11.17	0.00	4.26	3.50	1.99	0.00	0.00	0.00	0.00
Sensorless	lpm_gbm	216.47	257.56	178.31	117.01	90.70	83.90	73.50	65.95	61.57	57.97	56.54	57.15	55.45	66.24	68.24
	dt_gbm	<u>-0.01</u>	42.42	68.13	44.38	17.39	10.32	1.82	1.44	0.79	0.64	0.41	0.12	0.00	<u>-0.02</u>	0.34
senseit.aco	lpm_gbm	173.71	170.68	63.95	44.20	33.49	22.99	19.14	13.50	10.29	7.59	6.26	5.92	5.30	4.89	4.32
	dt_gbm	14.89	0.00	3.71	2.32	4.85	0.81	0.00	-	-	-	-	-	-	-	-
senseit.sei	lpm_gbm	160.59	65.27	23.44	10.48	6.76	4.86	4.82	4.46	4.79	4.12	4.54	5.17	3.91	4.21	4.46
	dt_gbm	2.66	1.01	3.49	2.29	0.95	1.30	1.37	0.00	-	-	-	-	-	-	-
covtype	lpm_gbm	36.87	49.24	12.78	11.21	7.84	7.15	7.15	8.07	7.70	8.25	10.94	8.35	4.37	8.77	5.84
	dt_gbm	342.27	92.85	43.23	20.04	8.14	8.05	5.67	3.26	4.92	3.52	2.72	0.00	0.00	0.00	1.74
connect-4	lpm_gbm	37.62	11.66	12.01	6.84	5.68	6.82	4.58	2.10	3.82	3.21	3.02	3.64	2.32	2.97	3.40
	dt_gbm	89.33	29.23	20.20	12.10	9.73	9.88	7.82	7.43	0.57	4.61	1.08	3.35	2.23	1.15	1.55

1. To compare improvements, we use the *Scaled Difference in Improvement (SDI)*:

$$SDI = \begin{cases} (\delta F1^{ora} - \delta F1^{den})/H, & \text{if } H > 0 \\ 0, & \text{if } H = 0 \end{cases} \quad (4)$$

where $H = \max\{\delta F1^{den}, \delta F1^{ora}\}$

Here $\delta F1^{ora}$ and $\delta F1^{den}$ are the improvements from our technique and by using density trees, respectively. The scaling wrt H ensures that $SDI \in [-1, 1]$ making it convenient to interpret. Note that $H \geq 0$ since both $\delta F1^{ora} \geq 0$ and $\delta F1^{den} \geq 0$ in the current scoring scheme. For brevity, we average the SDI scores at the level of a dataset, across model sizes, for a given model and oracle. This averaged score is denoted by \overline{SDI} , and this is what we report.

2. Since \overline{SDI} is aggregated over model sizes, we also report the percentage of times $\delta F1^{ora} > \delta F1^{den}$ across these model sizes. This is denoted as *pct_better*

All $\delta F1^{ora}$ and $\delta F1^{den}$ scores used are the *averaged over five runs*.

We consider our approach to be better if $\overline{SDI} > 0$ and *pct_better* > 50%. These scores are shown in Table 2. Since the density trees approach lacks a notion of an oracle, we present results for GBMs and RFs separately. Numbers that represent superior performance by density trees are underlined. Note also the two special groupings:

- **ANY**: For each model size, the SDI score considered is the higher of the ones obtained from using the GBM or RF as oracles. The \overline{SDI} and *pct_better* scores are computed based on these scores. This grouping represents the ideal way to use our technique in practice: try multiple oracles and pick the best.
- **OVERALL**: This averages results across datasets, to provide an aggregated view.

The cells identified by **OVERALL** and **ANY** provide comparison numbers aggregated over datasets, model sizes and oracles.

The predominance of non-underlined values indicate that our technique performs better in most settings. In both cases, the **OVERALL** + **ANY** entries indicate that our technique works better on average - in terms of both the extent of improvement \overline{SDI} and its frequency *pct_better*.

5 Multivariate Model Sizes

Our technique is applicable even when the model size has more than one attribute. This is because Algorithm 1 delegates size enforcement to $train_{\mathcal{L},g}$. Consider GBMs, where we might consider a bivariate size, $\eta = [max_depth, num_trees]$; here the quantities respectively denote the maximum depth allowed for each constituent DT in a GBM, and the number of DTs in the GBM. In Figure 3 we show how improvements for GBMs vary when $1 \leq max_depth \leq 5$ (x -axis) and $1 \leq num_trees \leq 5$

Table 2: LPM, DT compared to the Density Tree approach. All $\delta F1^{ora}$ and $\delta F1^{den}$ scores used are the *average over five runs*. Cases where density trees fare better are underlined. The line in the middle separates binary class datasets (top) from multi-class ones (bottom).

dataset	LPM			DT		
	GBM	RF	ANY	GBM	RF	ANY
cod-rna	-0.38, 0.00%	-0.45, 0.00%	-0.33, 0.00%	0.51, 60.00%	0.50, 70.00%	0.65, 80.00%
ijcnn1	0.06, 66.67%	0.11, 80.00%	0.20, 93.33%	0.23, 53.33%	0.68, 100.00%	0.68, 100.00%
higgs	-0.07, 40.00%	-0.07, 40.00%	0.04, 46.67%	0.23, 50.00%	0.61, 83.33%	0.61, 83.33%
covtype.binary	-0.16, 40.00%	-0.33, 13.33%	-0.15, 40.00%	0.23, 66.67%	0.26, 72.73%	0.38, 81.82%
phishing	0.30, 80.00%	0.37, 86.67%	0.38, 86.67%	0.11, 26.67%	-0.00, 26.67%	0.23, 46.67%
ala	-0.03, 60.00%	0.13, 66.67%	0.13, 66.67%	-0.06, 44.44%	0.43, 75.00%	0.52, 83.33%
pendigits	0.59, 100.00%	0.59, 93.33%	0.62, 100.00%	0.23, 60.00%	0.16, 46.67%	0.25, 60.00%
letter	0.79, 100.00%	0.81, 100.00%	0.81, 100.00%	0.02, 33.33%	-0.34, 13.33%	0.06, 40.00%
Sensorless	0.64, 100.00%	0.65, 100.00%	0.66, 100.00%	-0.23, 20.00%	-0.39, 20.00%	-0.23, 20.00%
senseit_aco	0.55, 100.00%	0.63, 100.00%	0.63, 100.00%	0.50, 85.71%	0.37, 75.00%	0.39, 75.00%
senseit_sei	0.61, 100.00%	0.66, 100.00%	0.67, 100.00%	-0.25, 42.86%	0.51, 100.00%	0.51, 100.00%
covtype	0.20, 80.00%	0.39, 93.33%	0.43, 100.00%	0.26, 66.67%	0.16, 66.67%	0.40, 80.00%
connect-4	0.23, 73.33%	0.24, 66.67%	0.38, 86.67%	-0.23, 33.33%	-0.13, 53.33%	0.08, 66.67%
OVERALL	0.28, 75.00%	0.32, 75.00%	0.37, 81.38%	0.10, 47.06%	0.16, 57.23%	0.31, 67.30%

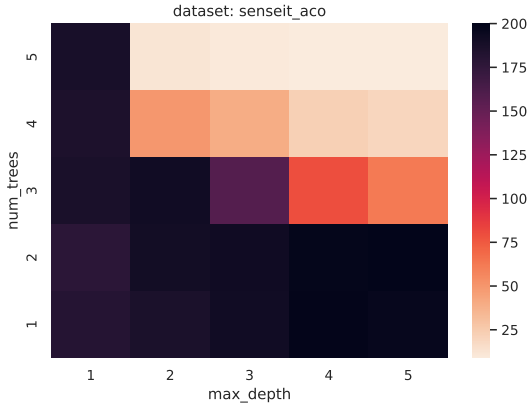


Figure 3: Improvements in test $F1$ -macro for the dataset *senseit-aco* for different sizes of *GBM* models. Here, model size is determined by both *max_depth* per tree and *number of trees*. Greater improvements are seen at lower sizes.

(*y*-axis); the oracle used is a *GBM* as well (unconstrained in size), and the dataset used is *senseit-aco*. The improvements are averaged over three runs. We observe the familiar pattern that as model sizes increase, in terms of both *max_depth* and *num_trees*, improvements decrease. Results over more datasets is visualized in §A.9.

6 Different Feature Spaces

So far we have assumed identical feature spaces for the interpretable and oracle models. But this is not necessary since all that is required of the oracle are uncertainty scores, irrespective of how the oracle arrives at them.

To highlight this, we consider the classification task of predicting nationalities from surnames (Rao and McMahan 2019). This dataset contains 18 nationalities. We use a *Gated Recurrent Unit (GRU)* (Cho et al. 2014) as our oracle. This is trained on the surnames presented as character sequences.

As the interpretable model, we use a *CART DT* that uses character *n*-grams as input. The improvements obtained are shown in Figure 4. This is practically powerful since it allows for translating information between models of varied capabilities. See §A.10 for additional details.

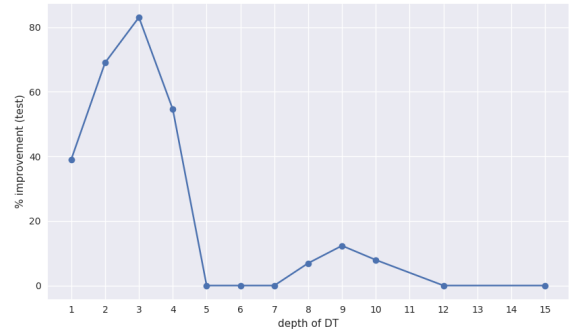


Figure 4: Improvements $\delta F1$ are shown for different depths of the *DT*.

7 Conclusion and Future work

In this work we presented a iterative model-agnostic technique to obtain good size-accuracy trade-offs. Conveniently, there is only one hyperparameter to set (the number of iterations). Further, it can accommodate multivariate model sizes and can be used with differing feature spaces between the oracle and the interpretable model. We believe that the strategy of manipulating the training distribution to improve accuracy presents multiple interesting possibilities.

For future work, we think the following ideas are promising: (a) A specialized version for differentiable models/losses. The current technique is attractive because of its broad applicability, but it can be made more efficient by exploiting differentiability (when possible). Techniques such as *bilevel optimization*, e.g., Pedregosa (2016), might be useful here to learn instance weights. (b) We noted that im-

provements diminish with increasing model size. An interesting direction to explore is whether this effect might be delayed by applying the technique separately to smaller models obtained from decomposing a larger model, e.g., subtrees within a larger tree.

References

- Alaa, A. M.; and van der Schaar, M. 2019. Demystifying Black-box Models with Symbolic Metamodels. In Wallach, H.; Larochelle, H.; Beygelzimer, A.; d'Alché-Buc, F.; Fox, E.; and Garnett, R., eds., *Advances in Neural Information Processing Systems*, volume 32. Curran Associates, Inc.
- Aldous, D. J. 1985. Exchangeability and related topics. In Hennequin, P. L., ed., *École d'Été de Probabilités de Saint-Flour XIII – 1983*, 1–198. Berlin, Heidelberg: Springer Berlin Heidelberg. ISBN 978-3-540-39316-0.
- Alimoglu, F.; and Alpaydin, E. 1996. Methods of Combining Multiple Classifiers Based on Different Representations for Pen-based Handwritten Digit Recognition. In *Proceedings of the Fifth Turkish Artificial Intelligence and Artificial Neural Networks Symposium (TAINN 96)*.
- Angwin, J.; Larson, J.; Mattu, S.; and Kirchner, L. 2016. Machine Bias. <https://www.propublica.org/article/machine-bias-risk-assessments-in-criminal-sentencing>.
- Baldi, P.; Sadowski, P.; and Whiteson, D. 2014. Searching for exotic particles in high-energy physics with deep learning. *Nature Communications*, 5(1): 4308.
- Benavoli, A.; Corani, G.; and Mangili, F. 2016. Should We Really Use Post-Hoc Tests Based on Mean-Ranks? *Journal of Machine Learning Research*, 17(5): 1–10.
- Bergstra, J.; Bardenet, R.; Bengio, Y.; and Kégl, B. 2011. Algorithms for Hyper-parameter Optimization. In *Proceedings of the 24th International Conference on Neural Information Processing Systems, NIPS'11*, 2546–2554. USA: Curran Associates Inc. ISBN 978-1-61839-599-3.
- Bergstra, J.; Yamins, D.; and Cox, D. D. 2013. Making a Science of Model Search: Hyperparameter Optimization in Hundreds of Dimensions for Vision Architectures. In *Proceedings of the 30th International Conference on International Conference on Machine Learning - Volume 28, ICML'13*, I–115–I–123. JMLR.org.
- Box, G. E. P.; and Cox, D. R. 1964. An Analysis of Transformations. *Journal of the Royal Statistical Society. Series B (Methodological)*, 26(2): 211–252.
- Breiman, L. 2001. Random Forests. *Machine Learning*, 45(1): 5–32.
- Breiman, L.; et al. 1984. *Classification and Regression Trees*. New York: Chapman & Hall. ISBN 0-412-04841-8.
- Brochu, E.; Cora, V. M.; and de Freitas, N. 2010. A Tutorial on Bayesian Optimization of Expensive Cost Functions, with Application to Active User Modeling and Hierarchical Reinforcement Learning. *CoRR*, abs/1012.2599.
- Caruana, R.; Lou, Y.; Gehrke, J.; Koch, P.; Sturm, M.; and Elhadad, N. 2015. Intelligible Models for HealthCare: Predicting Pneumonia Risk and Hospital 30-day Readmission. In *Proceedings of the 21th ACM SIGKDD International Conference on Knowledge Discovery and Data Mining, KDD '15*, 1721–1730. New York, NY, USA: ACM. ISBN 978-1-4503-3664-2.
- Chang, C.-C.; and Lin, C.-J. 2001. IJCNN 2001 Challenge: Generalization Ability and Text Decoding. In *In Proceedings of IJCNN. IEEE*, 1031–1036.
- Chang, C.-C.; and Lin, C.-J. 2011. LIBSVM: A library for support vector machines. *ACM Transactions on Intelligent Systems and Technology*, 2: 27:1–27:27. Software available at <http://www.csie.ntu.edu.tw/~cjlin/libsvm>.
- Chawla, N. V.; Bowyer, K. W.; Hall, L. O.; and Kegelmeyer, W. P. 2002. SMOTE: Synthetic Minority over-Sampling Technique. *J. Artif. Int. Res.*, 16(1): 321–357.
- Cho, K.; van Merriënboer, B.; Gulcehre, C.; Bahdanau, D.; Bougares, F.; Schwenk, H.; and Bengio, Y. 2014. Learning Phrase Representations using RNN Encoder–Decoder for Statistical Machine Translation. In *Proceedings of the 2014 Conference on Empirical Methods in Natural Language Processing (EMNLP)*, 1724–1734. Doha, Qatar: Association for Computational Linguistics.
- Collobert, R.; Bengio, S.; and Bengio, Y. 2002. A Parallel Mixture of SVMs for Very Large Scale Problems. In Dietterich, T. G.; Becker, S.; and Ghahramani, Z., eds., *Advances in Neural Information Processing Systems 14*, 633–640. MIT Press.
- Craven, M.; and Shavlik, J. 1995. Extracting Tree-Structured Representations of Trained Networks. In Touretzky, D.; Mozer, M.; and Hasselmo, M., eds., *Advances in Neural Information Processing Systems*, volume 8. MIT Press.
- Dean, D. J.; and Blackard, J. A. 1998. Comparison of neural networks and discriminant analysis in predicting forest cover types.
- Demšar, J. 2006. Statistical Comparisons of Classifiers over Multiple Data Sets. *Journal of Machine Learning Research*, 7(1): 1–30.
- Diaconis, P.; and Ylvisaker, D. 1983. Quantifying Prior Opinion. Technical Report EFS_NSF_207.
- Dua, D.; and Graff, C. 2017. UCI Machine Learning Repository.
- Duarte, M. F.; and Hu, Y. H. 2004. Vehicle Classification in Distributed Sensor Networks. *J. Parallel Distrib. Comput.*, 64(7): 826–838.
- Feldman, J. 2000. Minimization of Boolean complexity in human concept learning. *Nature*, 407: 630–3.
- Ferguson, T. S. 1973. A Bayesian Analysis of Some Non-parametric Problems. *The Annals of Statistics*, 1(2): 209 – 230.
- Friedman, J. H. 2001. Greedy function approximation: A gradient boosting machine. *The Annals of Statistics*, 29(5): 1189 – 1232.
- Garnett, R. 2023. *Bayesian Optimization*. Cambridge University Press.
- Ghose, A.; and Ravindran, B. 2020. Interpretability With Accurate Small Models. *Frontiers in Artificial Intelligence*, 3: 3.
- Good, J. H.; Kovach, T.; Miller, K.; and Dubrawski, A. 2023. Feature Learning for Interpretable, Performant Decision Trees. In *Thirty-seventh Conference on Neural Information Processing Systems*.

- Gou, J.; Yu, B.; Maybank, S. J.; and Tao, D. 2021. Knowledge Distillation: A Survey. *International Journal of Computer Vision*, 129(6): 1789–1819.
- Gunning, D. 2016. Explainable Artificial Intelligence. <https://www.darpa.mil/program/explainable-artificial-intelligence>.
- Guo, C.; Pleiss, G.; Sun, Y.; and Weinberger, K. Q. 2017. On Calibration of Modern Neural Networks. In *Proceedings of the 34th International Conference on Machine Learning - Volume 70, ICML'17*, 1321–1330. JMLR.org.
- He, H.; Bai, Y.; Garcia, E. A.; and Li, S. 2008. ADASYN: Adaptive synthetic sampling approach for imbalanced learning. In *2008 IEEE International Joint Conference on Neural Networks (IEEE World Congress on Computational Intelligence)*, 1322–1328.
- Herman, B. 2017. The Promise and Peril of Human Evaluation for Model Interpretability. Presented at NIPS 2017 Symposium on Interpretable Machine Learning. Available at: <https://arxiv.org/abs/1711.09889v3>.
- Herrewijnen, E.; Loerakker, M. B.; Vredenburg, M.; and Woźniak, P. W. 2024. Requirements and Attitudes towards Explainable AI in Law Enforcement. In *Proceedings of the 2024 ACM Designing Interactive Systems Conference, DIS '24*, 995–1009. New York, NY, USA: Association for Computing Machinery. ISBN 9798400705830.
- Hsu, C.-W.; and Lin, C.-J. 2002. A Comparison of Methods for Multiclass Support Vector Machines. *IEEE transactions on neural networks / a publication of the IEEE Neural Networks Council*, 13: 415–25.
- Ioffe, S.; and Szegedy, C. 2015. Batch Normalization: Accelerating Deep Network Training by Reducing Internal Covariate Shift. In *Proceedings of the 32nd International Conference on International Conference on Machine Learning - Volume 37, ICML'15*, 448–456. JMLR.org.
- J. Wang, Z.; Kale, A.; Nori, H.; Stella, P.; Nunnally, M. E.; Chau, D. H.; Vorvoreanu, M.; Wortman Vaughan, J.; and Caruana, R. 2022. Interpretability, Then What? Editing Machine Learning Models to Reflect Human Knowledge and Values. In *KDD 2022*.
- Japkowicz, N.; and Shah, M. 2011. *Evaluating Learning Algorithms: A Classification Perspective*. Cambridge University Press.
- Japkowicz, N.; and Stephen, S. 2002. The Class Imbalance Problem: A Systematic Study. *Intell. Data Anal.*, 6(5): 429–449.
- Jones, E.; Oliphant, T.; Peterson, P.; et al. 2001. SciPy: Open source scientific tools for Python. <http://www.scipy.org/>.
- Juan, Y.; Zhuang, Y.; Chin, W.-S.; and Lin, C.-J. 2016. Field-Aware Factorization Machines for CTR Prediction. In *Proceedings of the 10th ACM Conference on Recommender Systems, RecSys '16*, 43–50. New York, NY, USA: Association for Computing Machinery. ISBN 9781450340359.
- Ke, G.; Meng, Q.; Finley, T.; Wang, T.; Chen, W.; Ma, W.; Ye, Q.; and Liu, T.-Y. 2017. LightGBM: A Highly Efficient Gradient Boosting Decision Tree. In *Proceedings of the 31st International Conference on Neural Information Processing Systems, NIPS'17*, 3149–3157. USA: Curran Associates Inc. ISBN 978-1-5108-6096-4.
- Kulesza, T.; Stumpf, S.; Burnett, M.; Yang, S.; Kwan, I.; and Wong, W.-K. 2013. Too much, too little, or just right? Ways explanations impact end users' mental models. In *2013 IEEE Symposium on Visual Languages and Human Centric Computing*, 3–10.
- Lage, I.; Chen, E.; He, J.; Narayanan, M.; Kim, B.; Gershman, S. J.; and Doshi-Velez, F. 2019. Human Evaluation of Models Built for Interpretability. *Proceedings of the AAAI Conference on Human Computation and Crowdsourcing*, 7(1): 59–67.
- Lakkaraju, H.; Bach, S. H.; and Leskovec, J. 2016. Interpretable Decision Sets: A Joint Framework for Description and Prediction. In *Proceedings of the 22nd ACM SIGKDD International Conference on Knowledge Discovery and Data Mining, KDD '16*, 1675–1684. New York, NY, USA: ACM. ISBN 978-1-4503-4232-2.
- Larson, J.; Mattu, S.; Kirchner, L.; and Angwin, J. 2016. How We Analyzed the COMPAS Recidivism Algorithm. <https://www.propublica.org/article/how-we-analyzed-the-compas-recidivism-algorithm>.
- Lipton, Z. C. 2018. The Mythos of Model Interpretability. *Queue*, 16(3): 30:31–30:57.
- Lundberg, S. M.; and Lee, S.-I. 2017. A Unified Approach to Interpreting Model Predictions. In Guyon, I.; Luxburg, U. V.; Bengio, S.; Wallach, H.; Fergus, R.; Vishwanathan, S.; and Garnett, R., eds., *Advances in Neural Information Processing Systems 30*, 4765–4774. Curran Associates, Inc.
- Michie, D.; Spiegelhalter, D. J.; Taylor, C. C.; and Campbell, J., eds. 1995. *Machine Learning, Neural and Statistical Classification*. USA: Ellis Horwood. ISBN 013106360X.
- Mohammad, R. M.; Thabtah, F.; and McCluskey, L. 2012. An assessment of features related to phishing websites using an automated technique. In *2012 International Conference for Internet Technology and Secured Transactions*, 492–497.
- Mood, C. 2010. Logistic Regression : Why We Cannot Do What We Think We Can Do, and What We Can Do About It. *European Sociological Review*, 26(1): 67–82.
- Moustafa, N.; Koroniotis, N.; Keshk, M.; Zomaya, A. Y.; and Tari, Z. 2023. Explainable Intrusion Detection for Cyber Defences in the Internet of Things: Opportunities and Solutions. *IEEE Communications Surveys & Tutorials*, 25(3): 1775–1807.
- Murdoch, W. J.; Singh, C.; Kumbier, K.; Abbasi-Asl, R.; and Yu, B. 2019. Definitions, methods, and applications in interpretable machine learning. *Proceedings of the National Academy of Sciences*, 116(44): 22071–22080.
- Niculescu-Mizil, A.; and Caruana, R. 2005. Obtaining Calibrated Probabilities from Boosting. In *Proceedings of the Twenty-First Conference on Uncertainty in Artificial Intelligence, UAI'05*, 413–420. Arlington, Virginia, United States: AUAI Press. ISBN 0-9749039-1-4.
- Ohlssen, D. I.; Sharples, L. D.; and Spiegelhalter, D. J. 2007. Flexible random-effects models using Bayesian semi-parametric models: applications to institutional comparisons. *Statistics in Medicine*, 26(9): 2088–2112.

- Paschke, F.; Bayer, C.; Bator, M.; Mönks, U.; Dicks, A.; Enge-Rosenblatt, O.; and Lohweg, V. 2013. Sensorlose Zustandsüberwachung an Synchronmotoren. In *Proceedings of Computational Intelligence Workshop*.
- Pedregosa, F. 2016. Hyperparameter Optimization with Approximate Gradient. In *Proceedings of the 33rd International Conference on International Conference on Machine Learning - Volume 48, ICML'16*, 737–746. JMLR.org.
- Pedregosa, F.; Varoquaux, G.; Gramfort, A.; Michel, V.; Thirion, B.; Grisel, O.; Blondel, M.; Prettenhofer, P.; Weiss, R.; Dubourg, V.; Vanderplas, J.; Passos, A.; Cournapeau, D.; Brucher, M.; Perrot, M.; and Duchesnay, E. 2011. Scikit-learn: Machine Learning in Python. *Journal of Machine Learning Research*, 12: 2825–2830.
- Piltaver, R.; Luštrek, M.; Gams, M.; and Martinčić-Ipšić, S. 2016. What makes classification trees comprehensible? *Expert Systems with Applications*, 62: 333–346.
- Platt, J. 1998. Fast Training of Support Vector Machines Using Sequential Minimal Optimization. In *Advances in Kernel Methods - Support Vector Learning*. MIT Press.
- Platt, J. C. 1999. Probabilistic Outputs for Support Vector Machines and Comparisons to Regularized Likelihood Methods. In *ADVANCES IN LARGE MARGIN CLASSIFIERS*, 61–74. MIT Press.
- Poursabzi-Sangdeh, F.; Goldstein, D.; Hofman, J.; Wortman Vaughan, J.; and Wallach, H. 2021. Manipulating and Measuring Model Interpretability. In *CHI 2021*.
- Prokhorov, D. 2001. IJCNN 2001 Neural Network Competition. <http://www.geocities.ws/ijcnn/nnc-ijcnn01.pdf>.
- Rao, D.; and McMahan, B. 2019. *Natural Language Processing with PyTorch*. O'Reilly. ISBN 978-1491978238. <https://www.amazon.com/Natural-Language-Processing-PyTorch-Applications/dp/1491978236/> and <https://github.com/joosthub/PyTorchNLPBook>.
- Ribeiro, M. T.; Singh, S.; and Guestrin, C. 2016. “Why Should I Trust You?”: Explaining the Predictions of Any Classifier. In *Proceedings of the 22Nd ACM SIGKDD International Conference on Knowledge Discovery and Data Mining, KDD '16*, 1135–1144. New York, NY, USA: ACM. ISBN 978-1-4503-4232-2.
- Santhiappan, S.; Chelladurai, J.; and Ravindran, B. 2018. A Novel Topic Modeling Based Weighting Framework for Class Imbalance Learning. In *Proceedings of the ACM India Joint International Conference on Data Science and Management of Data, CoDS-COMAD '18*, 20–29. New York, NY, USA: Association for Computing Machinery. ISBN 9781450363419.
- Santurkar, S.; Tsipras, D.; Ilyas, A.; and Madry, A. 2018. How Does Batch Normalization Help Optimization? In Bengio, S.; Wallach, H.; Larochelle, H.; Grauman, K.; Cesa-Bianchi, N.; and Garnett, R., eds., *Advances in Neural Information Processing Systems*, volume 31. Curran Associates, Inc.
- Scheffer, T.; Decomain, C.; and Wrobel, S. 2001. Active Hidden Markov Models for Information Extraction. In *Proceedings of the 4th International Conference on Advances in Intelligent Data Analysis, IDA '01*, 309–318. London, UK, UK: Springer-Verlag. ISBN 3-540-42581-0.
- Settles, B. 2009. Active Learning Literature Survey. Computer Sciences Technical Report 1648, University of Wisconsin–Madison.
- Shahriari, B.; Swersky, K.; Wang, Z.; Adams, R. P.; and de Freitas, N. 2016. Taking the Human Out of the Loop: A Review of Bayesian Optimization. *Proceedings of the IEEE*, 104(1): 148–175.
- Sturges, H. A. 1926. The Choice of a Class Interval. *Journal of the American Statistical Association*, 21(153): 65–66.
- Tibshirani, R. 1996. Regression Shrinkage and Selection via the Lasso. *Journal of the Royal Statistical Society. Series B (Methodological)*, 58(1): 267–288.
- Tjoa, E.; and Guan, C. 2021. A Survey on Explainable Artificial Intelligence (XAI): Toward Medical XAI. *IEEE Transactions on Neural Networks and Learning Systems*, 32(11): 4793–4813.
- Ustun, B.; and Rudin, C. 2016. Supersparse linear integer models for optimized medical scoring systems. *Machine Learning*, 102(3): 349–391.
- Uzilov, A. V.; Keegan, J. M.; and Mathews, D. H. 2006. Detection of non-coding RNAs on the basis of predicted secondary structure formation free energy change. *BMC bioinformatics*, 7: 173–173. 16566836[pmid].
- Wang, C.-C.; Tan, K. L.; Chen, C.-T.; Lin, Y.-H.; Keerthi, S. S.; Mahajan, D.; Sundararajan, S.; and Lin, C.-J. 2018. Distributed Newton Methods for Deep Neural Networks. *Neural Comput.*, 30(6): 1673–1724.
- Wilcoxon, F. 1945. Individual Comparisons by Ranking Methods. *Biometrics Bulletin*, 1(6): 80–83.
- Yeo, I.-K.; and Johnson, R. A. 2000. A New Family of Power Transformations to Improve Normality or Symmetry. *Biometrika*, 87(4): 954–959.

8 Reproducibility checklist

This paper:

- Includes a conceptual outline and/or pseudocode description of AI methods introduced. Yes.
- Clearly delineates statements that are opinions, hypothesis, and speculation from objective facts and results. Yes.
- Provides well marked pedagogical references for less-familiar readers to gain background necessary to replicate the paper. Yes.

Does this paper make theoretical contributions? No.

If yes, please complete the list below.

- All assumptions and restrictions are stated clearly and formally. NA.
- All novel claims are stated formally (e.g., in theorem statements). NA.
- Proofs of all novel claims are included. NA.
- Proof sketches or intuitions are given for complex and/or novel results. NA.

- Appropriate citations to theoretical tools used are given. NA.
- All theoretical claims are demonstrated empirically to hold. NA.
- All experimental code used to eliminate or disprove claims is included. NA.

Does this paper rely on one or more datasets? Yes.

If yes, please complete the list below.

- A motivation is given for why the experiments are conducted on the selected datasets. Yes.
- All novel datasets introduced in this paper are included in a data appendix. NA.
- All novel datasets introduced in this paper will be made publicly available upon publication of the paper with a license that allows free usage for research purposes. NA.
- All datasets drawn from the existing literature (potentially including authors' own previously published work) are accompanied by appropriate citations. Yes.
- All datasets drawn from the existing literature (potentially including authors' own previously published work) are publicly available. Yes.
- All datasets that are not publicly available are described in detail, with explanation why publicly available alternatives are not scientifically satisfying. NA.

Does this paper include computational experiments? Yes.

If yes, please complete the list below.

- Any code required for pre-processing data is included in the appendix. Yes.
- All source code required for conducting and analyzing the experiments is included in a code appendix. Yes.
- All source code required for conducting and analyzing the experiments will be made publicly available upon publication of the paper with a license that allows free usage for research purposes. Yes.
- All source code implementing new methods have comments detailing the implementation, with references to the paper where each step comes from. Yes.
- If an algorithm depends on randomness, then the method used for setting seeds is described in a way sufficient to allow replication of results. Yes.
- This paper specifies the computing infrastructure used for running experiments (hardware and software), including GPU/CPU models; amount of memory; operating system; names and versions of relevant software libraries and frameworks. Yes.
- This paper formally describes evaluation metrics used and explains the motivation for choosing these metrics. Yes.
- This paper states the number of algorithm runs used to compute each reported result. Yes.
- Analysis of experiments goes beyond single-dimensional summaries of performance (e.g., average; median) to include measures of variation, confidence, or other distributional information. Yes.

- The significance of any improvement or decrease in performance is judged using appropriate statistical tests (e.g., Wilcoxon signed-rank). Yes.
- This paper lists all final (hyper-)parameters used for each model/algorithm in the paper's experiments. Yes.
- This paper states the number and range of values tried per (hyper-) parameter during development of the paper, along with the criterion used for selecting the final parameter setting. Yes.

A Appendix

A.1 Uncertainty Metrics

Some other popular uncertainty metrics are:

1. **Least confident:** we calculate the extent of uncertainty w.r.t. the class we are most confident about:

$$u_M(x) = 1 - \max_{y_i \in \{1, 2, \dots, C\}} M(y_i | x) \quad (5)$$

Here, we have C classes, and $M(y_i | x)$ is the probability score produced by the model¹⁰.

2. **Entropy:** this is the standard Shannon entropy measure calculated over class prediction confidences:

$$u_M(x) = - \sum_{y_i \in \{1, 2, \dots, C\}} M(y_i | x) \log M(y_i | x) \quad (6)$$

We do not use the *least confident* metric since it completely ignores confidence distribution across labels. While *entropy* is quite popular, and does take into account the confidence distribution, we do not use it since it reaches its maximum for only points for which the classifier must be equally ambiguous about *all* labels; for datasets with many labels (one of our experiments uses a dataset with 26 labels - see Table 4) we may never reach this maximum.

Fig 5 visually shows what uncertainty values look like for the different metrics. Panel (a) displays a dataset with 4 labels. A probabilistic *linear Support Vector Machine (SVM)* is learned on this, and uncertainty scores corresponding to the metrics “margin”, “least confident” and “entropy” are visualized in panels (b), (c) and (d) respectively. Darker shades of gray correspond to high uncertainty. Observe that only the “margin” metric in panel (b) achieves scores close to 1 at the two-label boundaries.

There is no best uncertainty metric in general, and the choice is usually application specific (Settles 2009).

A.2 Sampling from the IBMM

Given our representation, the procedure to sample N_s points, from a dataset D , using an oracle M_O is shown in Algorithm 2. We also explain the steps below:

1. Determine partitioning over the N_s points induced by the DP . We use the *Chinese Restaurant Process* (Aldous 1985) for this. Let’s assume this step produces k partitions $\{c_1, c_2, \dots, c_k\}$ and quantities $n_i \in \mathbb{N}$ where $\sum_{i=1}^k n_i = N$. Here, n_i denotes the number of points that belong to partition c_i .
2. We determine the $Beta(A_i, B_i)$ component for each c_i by sampling from the priors, i.e., $A_i \sim \text{scale} \times Beta(a, b)$ and $B_i \sim \text{scale} \times Beta(a', b')$.
3. Repeat for each c_i : for each instance-label pair (x_j, y_j) in our training dataset, we calculate the oracle uncertainty score, $u_{M_O}(x_j)$. We then calculate $p_j = c \cdot$

¹⁰The possibly confusing name “least confident” for this idea originated within the context of uncertainty sampling, where we are interested in sampling the most uncertain point, $x^* = \arg \min_x [\max_{y_i \in \{1, 2, \dots, C\}} M(y_i | x)]$, which may be considered to be the instance with the “least most confident label”.

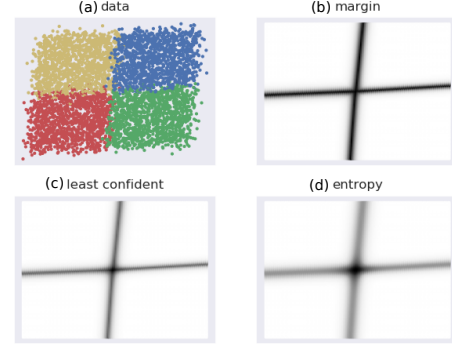


Figure 5: Visualizations of different uncertainty metrics. (a) shows a 4-label dataset on which linear SVM is learned. (b), (c), (d) visualize uncertainty scores based on different metrics, as per the linear SVM, where darker shades imply higher scores.

$Beta(u_{M_O}(x_j) | A_i, B_i)$. c is a normalizing constant that scales the probabilities across instances to sum to 1. The quantities p_j are used as sampling probabilities for various (x_j, y_j) , and n_i points are sampled with replacement based on them.

A.3 Default Parameters

The optimizer we use, TPE, requires *box constraints*. Here we specify our search space for the optimization variables, Φ in Algorithm 1:

1. p_o : We want to allow the algorithm to pick an arbitrary fraction of samples from the original data; we set $p_o \in [0, 1]$.
2. N_s : We set $N_s \in [400, 10000]$. The lower bound ensures we have statistically significant results. The upper bound is set to a reasonably large value.
3. $\{a, b, a', b'\}$: Each of these parameters are allowed a range $[0.1, 10]$ to allow for a wide range of shapes for the component $Beta$ distributions.
4. $scale$: We fix $scale = 10000$ for our experiments, to allow for A_i and B_i to model skewed distributions where shape parameter large values might be required. For small values, the algorithm adapts by learning the appropriate $\{a, b, a', b'\}$.
5. α : For a DP, $\alpha \in \mathbb{R}_{>0}$. We use a lower bound of 0.1.

To determine the upper bound, we rely on the following empirical relationship (Ohlssen, Sharples, and Spiegelhalter 2007) between the number of components k and α :

$$E[k | \alpha] \approx 5\alpha + 2 \quad (7)$$

We empirically estimated a fairly inclusive upper bound on the number of components to be 500, which provides us the α upper bound of 99.6. Thus, we use $\alpha \in [0.1, 99.6]$.

Algorithm 2: Sample based on uncertainties and Ψ

Data: Sample size N_s , oracle M_O , dataset $D = \{(x_i, y_i)\}_{i=1}^N$, IBMM parameters $\Psi = \{\alpha, a, b, a', b'\}$

Result: Sample D' , where $|D'| = N_s$

```
1  $D' = \{\}$  // assumed to be a multiset
2  $\{(c_1, n_1), (c_2, n_2), \dots, (c_k, n_k)\} \leftarrow$  partition  $N_s$ 
   using the DP // Here  $\sum_{i=1}^k n_i = N_s$ .
3 for  $i \leftarrow 1$  to  $k$  do
4    $A_i \sim \text{scale} \times \text{Beta}(a, b)$ 
5    $B_i \sim \text{scale} \times \text{Beta}(a', b')$ 
6   for  $j \leftarrow 1$  to  $N$  do
7      $p_j \leftarrow c \cdot \text{Beta}(u_{M_O}(x_j); A_i, B_i)$  //  $c$  is
       a normalizing constant s.t.  $\sum_{i=1}^N c \cdot p_j = 1$ .
8   end
9    $\text{temp} \leftarrow$  sample with replacement  $n_i$ 
     instance-label pairs based on  $p_j$ 
10   $D' \leftarrow D' \uplus \text{temp}$  //  $\uplus$  is the multiset
     sum
11 end
12 return  $D'$ 
```

A.4 Notes on the Main Algorithm

We provide some additional details in reference to the main algorithm - Algorithm 1 - in the paper. For convenience, we reproduce the algorithm here, as Algorithm 3. Our notes follow:

1. We will consider the initialization to happen at $t = 0$, while the iterations range from 1 to T . Φ_0 is set to: $\alpha = 0.1, a = 1, b = 1, a' = 1, b' = 1, N_s = |D_{\text{train}}|, p_o = 1$. A model is constructed based on Φ_0 and a score s_0 is recorded. (Φ_0, s_0) serve as the history for the iteration at $t = 1$. The values for α, a, b, a', b' carry no significance and are arbitrary, since setting $p_o \rightarrow 1$ forces sampling only from the original distribution. Combined with $N_s = |D_{\text{train}}|$, this setting mimics the baseline, i.e., training the interpretable model without our algorithm, thus providing the optimizer with a good initial reference point in its search space.
2. The optimizer is represented by the function call $\text{suggest}()$ which takes as input all past parameter values and validation scores. $\text{suggest}()$ denotes a generic optimizer; not all optimizers require this extent of historical information.
3. While the training algorithm for the oracle, $\text{train}_{O,h}()$ is taken as input, a pre-constructed oracle M_O may also be used. This would eliminate the oracle training step in line 2.
4. $\text{acc}()$ on the validation data, D_{val} , serves as both the objective and fitness function.
5. Evaluation on the test set, D_{test} is done only once, in line 16, with the model that produces the best validation score.

Algorithm 3: Learning interpretable model using oracle - reproduction of Algorithm 1.

Data: Dataset D , model size η , $\text{train}_{O,h}()$, $\text{train}_{\mathcal{I},g}()$, iterations T

Result: Optimal parameters Φ^* , test set accuracy s_{test} at Φ^* , and interpretable model M^* at Φ^*

```
1 Create splits  $D_{\text{train}}, D_{\text{val}}, D_{\text{test}}$  from  $D$ , stratified
  wrt labels. Here  $|D_{\text{train}}| : |D_{\text{val}}| : |D_{\text{test}}| :: 60 : 20 : 20$ .
2  $M_O \leftarrow \text{train}_{O,h}(D_{\text{train}}, *)$ 
3 for  $t \leftarrow 1$  to  $T$  do
4    $\Phi_t \leftarrow \text{suggest}(s_0, s_1, \dots, s_{t-1}, \Phi_0, \Phi_1, \dots, \Phi_{t-1})$ 
     //  $s_0, \Phi_0$  initialized at  $t = 0$ , see text. Note:
      $\Phi_t = \{\Psi_t, N_{s,t}, p_{o,t}\}$  where  $\Psi_t = \{\alpha_t, a_t, b_t, a'_t, b'_t\}$ .
5    $N_o \leftarrow p_{o,t} \times N_{s,t}$ 
6    $N_u \leftarrow N_{s,t} - N_o$ 
7    $D_o \leftarrow$  uniformly sample with replacement  $N_o$ 
     points from  $D_{\text{train}}$ 
8    $D_u \leftarrow$  sample  $N_u$  points from  $D_{\text{train}}$  using the
     DP-based IBMM given current values for  $N_u, M_O, D_{\text{train}}, \Psi_t$  // see Algorithm
     A.2 for details
9    $D_s \leftarrow D_o \uplus D_u$  //  $D_o, D_u$  are assumed
     to be multisets
10   $M_t \leftarrow \text{train}_{\mathcal{I},g}(D_s, \eta)$ 
11   $s_t \leftarrow \text{acc}(M_t, D_{\text{val}})$ 
12 end
13  $t^* \leftarrow \arg \max_t \{s_1, s_2, \dots, s_{T-1}, s_T\}$ 
14  $\Phi^* \leftarrow \Phi_{t^*}$ 
15  $M^* \leftarrow M_{t^*}$ 
16  $s_{\text{test}} \leftarrow \text{acc}(M^*, D_{\text{test}})$ 
17 return  $\Phi^*, s_{\text{test}}, M^*$ 
```

6. Since we sample with replacement, both temporary datasets D_o and D_u , procured from uniformly sampling the original training data and sampling based on uncertainties respectively, are multisets. Accordingly, line 9 uses the multiset sum operator \uplus to combine them.
7. M_t is created (line 10) with limited or no hyperparameter search using simple random validation, i.e., a stratified (by labels) random sample of size $0.2N_{s,t}$ is used as the validation set. A restricted search is performed because often hyperparameters are correlated with model size, and setting them to particular values would fail to produce a model of the required size η . As an example, consider DTs: setting a high threshold for the number of instances in a node for it be split (hyperparameter `min_samples_split` in *scikit-learn*'s (Pedregosa et al. 2011) implementation) would produce only short trees.

We don't use cross-validation since at small values of $N_{s,t}$, the amount of training data, i.e., $(\frac{k-1}{k})N_{s,t}$ for k -folds, may become too small to obtain a good model. For example, for 3-folds, the training data size is $0.67N_{s,t}$.

The data shortage problem can be addressed by increasing the number of folds, but that also increases the running time per iteration owing to the larger number of models that now need to be trained. As a practical compromise, we perform simple validation *thrice* and average the outcomes. This number is configurable, and may be decreased for models that are expensive to train.

8. Since the validation score s_t (line 11) needs to be reliable, in our implementation we repeat lines 7-10 *thrice* and use the averaged validation score as s_t .
9. Class imbalance is accounted for in our implementation when training model M_t in line 10. We either balance the data by sampling (this is the case with a *Linear Probability Model*), or an appropriate cost function is used to simulate balanced classes (this is the case with DTs and GBMs).

It is important to note here that D_{val} and D_{test} are not modified by our algorithm in any way, and therefore s_t and s_{test} measure the accuracy on the original distribution.

A.5 Smoothing the Optimization Landscape

A practical consideration in our implementation is if we might facilitate finding the maxima Φ^* in Algorithm 1?

Since BayesOpt algorithms model the response surface of the actual objective function using a finite number of evaluations (s_t in Algorithm 1), a certain degree of *smoothness* is assumed (Shahriari et al. 2016; Brochu, Cora, and de Freitas 2010). Here, the optimization variables Φ influence the objective value s via this indirect chain: $\Phi_t \rightarrow D_s \rightarrow M_t \rightarrow s_t$ (symbols as in Algorithm 1), and for BayesOpt to work well, it is required that small changes in Φ_t result in small changes in s_t .

However, we have noticed that an oracle might produce uncertainty score distributions that are “spiky” or “jagged” - as an example, see the curve labelled “original” in Figure 6(a); which leads us to hypothesize that this principle is violated in general. A spiky distribution implies that small shifts $\Phi_t + \Delta\Phi_t$ may lead to sampling of instances with very different uncertainties; and since such instances may occur in regions far from those indicated by Φ_t , they produce models with different class prediction behavior. This indirectly causes a disproportionate shift in s_t . While, in theory, a good BayesOpt algorithm should adapt to such problem characteristics, in practice they make the optimization problem harder, especially when the optimization budget is small.

To address this, we “flatten” the distribution¹¹ within $[0, 1]$. Our transformation is simple: we divide the interval $[0, 1]$ into B bins, and map approximately $|D_{train}|/B$ uncertainty scores to each bin, while maintaining order between the original and mapped scores. Within a bin, the mapped scores are linearly spread across its range. This distributes

¹¹Distribution transformations have a long history in statistics, e.g., *power transforms* like the *Box-Cox* (Box and Cox 1964) and *Yeo-Johnson* (Yeo and Johnson 2000) transforms. Within ML, *Batch Normalization* (Ioffe and Szegedy 2015) is a popular example of a distribution transformation applied to a loss landscape (Santurkar et al. 2018).

the mapped scores approximately uniformly in the range $[0, 1]$. The algorithm is detailed in Algorithm 4.

Algorithm 4: Flatten distribution of uncertainty scores $\{u(x_1), u(x_2), \dots, u(x_N)\}$

Data: $\{u(x_1), u(x_2), \dots, u(x_N)\}$, number of bins B
Result: $\{u'(x_1), u'(x_2), \dots, u'(x_N)\}$

- 1 $bin_size \leftarrow \lceil N/B \rceil, bin_range \leftarrow 1/B$
- 2 $bin_min \leftarrow [], bin_max \leftarrow []$
- 3 Let $sortedIndex(i) \in \{1, 2, \dots, N\}$ be the index of $u(x_i)$ in the sequence of scores ordered by non-decreasing values.
- 4 **for** $j \leftarrow 1$ **to** B **do**
- 5 $bin_min[j] \leftarrow \min\{u(x_i) | i \in \{1, 2, \dots, N\} \wedge sortedIndex(i) = j\}$
- 6 $bin_max[j] \leftarrow \max\{u(x_i) | i \in \{1, 2, \dots, N\} \wedge sortedIndex(i) = j\}$
- 7 **end**
- 8 **for** $i \leftarrow 1$ **to** N **do**
- 9 $j \leftarrow sortedIndex(i)$
- 10 $bin_num \leftarrow \lceil j/bin_size \rceil$
- 11 $boundary_low \leftarrow (bin_num - 1) \times bin_range + \delta$
- 12 $boundary_high \leftarrow bin_num \times bin_range - \delta$
- 13 $u'(x_i) \leftarrow low + \frac{u(x_i) - bin_min[j]}{bin_max[j] - bin_min[j]} \times (boundary_high - boundary_low)$
- 14 **end**
- 15 **return** $\{u'(x_1), u'(x_2), \dots, u'(x_N)\}$

Figure 6 visualizes the process of flattening. The original and modified uncertainty distributions for the datasets *Sensorless* and *covtype.binary* are shown in Figure 6(a) and 6(b) respectively.

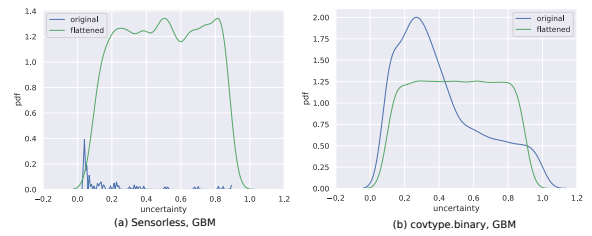


Figure 6: Example of curve-flattening, for datasets (a) *Sensorless* and (b) *covtype.binary*. The uncertainty scores shown are obtained using the *GBM* oracle.

While *Sensorless* appears to have a non-smooth distribution, and flattening here might help, this seems redundant for *covtype.binary*. However, since this step is computationally cheap, we perform this for all our experiments, saving us the effort of assessing its need.

Our transformation is invertible, which is useful in analyzing the observations from our experiments. Note however, it is not differentiable because of the discontinuities at the bin-boundaries; we also don’t require this property.

The transformation affects line 7 in Algorithm 2. Instead of sampling based on the actual oracle uncertainty scores:

Table 3: Improved scores averaged over three trials, shown for different parameter settings, with and without flattening. Here, Setting 1 is $\{max_components = 500, scale = 10000\}$ and Setting 2 is $\{max_components = 50, scale = 10\}$. “curr.” signifies this is the current setting for our experiments in the main paper, while “low” signifies lower values of parameters. Highlighted cells indicate positive effect of flattening.

dataset	dist.	Setting 1 (curr.)			Setting 2 (low)		
		1	2	3	1	2	3
Sensorless	original	0.39	0.54	0.57	0.38	0.42	0.41
	flattened	0.44	0.53	0.55	0.43	0.54	0.59
covtype.binary	original	0.66	0.69	0.71	0.64	0.66	0.71
	flattened	0.68	0.73	0.73	0.65	0.71	0.71

$$p_j \leftarrow \text{Beta}(u_{M_O}(x_j); A_i, B_i) \quad (8)$$

we sample based on the transformed uncertainty scores, $u'_{M_O}(x_j)$:

$$p_j \leftarrow \text{Beta}(u'_{M_O}(x_j); A_i, B_i) \quad (9)$$

In §A.6 we show that smoothing indeed has a positive effect.

A.6 Effect of Smoothing

We first consider the question: does flattening (§A.5) help? Table 3 contrasts *improved F1* scores obtained without (rows denoted as “original”) and with (denoted “flattened”) flattening the uncertainty distribution. This is shown for the datasets `Sensorless` and `covtype.binary`, for model $size \in \{1, 2, 3\}$, with $model = LPM$ and $oracle = GBM$. Two different parameter settings are used: (a) In Setting 1, maximum allowed *Beta* components are 500 and $scale = 10000$ (b) Setting 2 looks at much lower values of these parameters where maximum allowed components is 50 and $scale = 10$. The scores presented are the average over three trials.

We observe that while flattening influences results, other parameters determine the magnitude of its effect. At Setting 1, `Sensorless` is affected at $size = 1$ (flattening is better), but at higher sizes the differences seem to be from random variations across trials. At Setting 2 however, the differences are seen for $size \in \{1, 2, 3\}$ (flattening is better). For `covtype.binary` only $size = 2$ seems to be affected in either setting.

Recall we had noted in Figure 6 that the datasets `Sensorless` and `covtype.binary` have non-smooth and smooth uncertainty distributions respectively. The observations in Table 3 align well with the expectation that `Sensorless` is positively affected by the transformation, while results for `covtype.binary` remain mostly unchanged.

Based on these tests, we hypothesize that for non-smooth uncertainty distributions, flattening makes our technique robust across parameter settings. It does not affect smooth distributions in a significant way. Of course, rigorous and extensive tests are required to conclusively establish this effect.

A.7 Datasets

Table 4 provides details about the various datasets used in the experiments in §4. All of these are publicly available on the *LIBSVM* website (Chang and Lin 2011).

The “Label Entropy” column indicates how balanced a dataset is wrt its classes. For a dataset with N instances and C labels, this is calculated as:

$$\text{Label Entropy} = \sum_{j \in \{1, 2, \dots, C\}} -p_j \log_C p_j \quad (10)$$

$$\text{Here, } p_j = \frac{|\{x_i | y_i = j\}|}{N}$$

Label Entropy $\in [0, 1]$, where values close to 1 denote the dataset is nearly balanced, and values close to 0 represent relative imbalance.

A.8 Validation Results

An extended version of the results shown in Table 1 are presented here in Table 5. This shows results for all combinations of models and oracles: $\{LPM, DT\} \times \{GBM, RF\}$.

We also perform a *Wilcoxon signed-rank test* (Wilcoxon 1945) to measure statistical significance. We use this test as it has been shown to be useful in comparing classifiers (Demšar 2006; Benavoli, Corani, and Mangili 2016; Japkowicz and Shah 2011). Results are shown in figure 7 for the following test setup:

1. We divide the analysis by model size. This is because size strongly influences $\delta F1$ (as in Table 5).
2. Normalized model sizes are used. Binning of model sizes is done using *Sturges rule* (Sturges 1926).
3. The *one-sided* version of the *paired* test is performed for each bin, where pairs of scores $F1^{base}$ and $F1^*$ for a dataset, for models with sizes assigned to the bin, are compared. In cases where multiple model sizes for a dataset fall within the same bin, $F1^{base}$ and $F1^*$ are first averaged and then compared.
4. The following hypotheses are tested:
 - H_0 , null hypothesis: accuracies of models produced by our technique are not better.
 - H_1 , alternate hypothesis: accuracies of models trained using the oracle are better.

p -values are shown for each bin. Small p -values favor H_1 , i.e., our algorithm.
5. Scores of $\delta F1 = 0$ are split equally between positive and negative ranks¹².

A.9 Multivariate Model Sizes

As a continuation of the result shown in §5, we show results on the datasets (a) *senseit-sei* (b) *higgs* (c) *cod-rna* and (d) *senseit-aco* here. We continue to observe pattern that as model sizes increase, in terms of both max_depth and num_trees , improvements decrease.

¹²The `zsplit` option in https://numpy.org/doc/stable/reference/generated/numpy.histogram_bin_edges.html is used.

Table 4: We use the following datasets available on the LIBSVM website (Chang and Lin 2011). Their original source is mentioned in the “Description” column. 10000 instances from each dataset are used. A $train : val : test$ split ratio of 60 : 20 : 20 is used for D_{train} , D_{val} and D_{test} in Algorithm 1. The splits are stratified wrt labels.

S.No.	Dataset	Dimensions	# Classes	Label Entropy	Description
1	cod-rna	8	2	0.92	Predict presence of non-coding RNA common to a pair of RNA sequences, based on individual sequence properties and their similarity (Uzilov, Keegan, and Mathews 2006).
2	ijcnn1	22	2	0.46	Time series data produced by an internal combustion engine is used to predict normal engine firings vs misfirings (Prokhorov 2001). Transformations as in Chang and Lin (2001).
3	higgs	28	2	1.00	Predict if a particle collision produces Higgs bosons or not, based on collision properties (Baldi, Sadowski, and Whiteson 2014).
4	covtype.binary	54	2	1.00	Modification of the <i>covtype</i> dataset (see row 12), where classes are divided into two groups (Collobert, Bengio, and Bengio 2002).
5	phishing	68	2	0.99	Various website features are used to predict if the website is a <i>phishing</i> website (Mohammad, Thabtah, and McCluskey 2012). Transformations used as in Juan et al. (2016)
6	ala	123	2	0.80	Predict whether a person makes over 50K a year, based on census data variables (Dua and Graff 2017). Transformations as in (Platt 1998).
7	pendigits	16	10	1.00	Classify handwritten digit samples into the digits 0-9 (Alimoglu and Alpaydin 1996; Dua and Graff 2017).
8	letter	16	26	1.00	Images of the capital letters A-Z were produced by random distortion of these characters from 20 fonts. The task is to classify these character images as one of the original letters (Michie et al. 1995). Transformations as in (Hsu and Lin 2002).
9	Sensorless	48	11	1.00	Based on phase current measurements of an electric motor, predict different error conditions (Paschke et al. 2013). We use the transformations from (Wang et al. 2018).
10	senseit_aco	50	3	0.95	Predict vehicle type using acoustic data gathered by a sensor network (Duarte and Hu 2004).
11	senseit_sei	50	3	0.94	Predict vehicle type using seismic data gathered by a sensor network (Duarte and Hu 2004).
12	covtype	54	7	0.62	Predict forest cover type from cartographic variables (Dean and Blackard 1998; Dua and Graff 2017).
13	connect-4	126	3	0.77	Predict if the first player wins, loses or draws, based on board positions of the board game <i>Connect Four</i> (Dua and Graff 2017).

Table 5: This table shows the average improvements, $\delta F1$, over five runs for different combinations of models and oracles: $\{LPM, DT\} \times \{GBM, RF\}$. This is an extended version of the results in Table 1. The improvements are measured relative to the model at the first iteration. The best improvement for a model size and oracle is indicated in bold. Here, $\delta F1 \in (-\infty, \infty)$. Negative improvements are shown in underlined.

dataset	model_ora	1	2	3	4	5	6	7	8	9	10	11	12	13	14	15
cod-rna	lpm_gbm	1.39	12.53	14.76	15.73	14.97	12.00	0.00	0.08	-	-	-	-	-	-	-
	lpm_rf	2.66	13.91	14.69	15.34	16.06	12.49	8.30	0.00	-	-	-	-	-	-	-
	dt_gbm	0.00	0.00	0.00	1.26	0.00	0.00	0.00	0.00	<u>-0.28</u>	0.08	-	-	-	-	-
	dt_rf	0.00	0.00	1.78	2.28	0.39	<u>-0.02</u>	0.17	0.47	0.00	0.72	-	-	-	-	-
ijcnn1	lpm_gbm	<u>-0.16</u>	3.36	3.93	0.00	5.19	4.18	3.85	3.79	3.69	2.99	2.97	3.21	3.11	3.26	3.02
	lpm_rf	0.19	2.80	3.36	3.65	3.33	1.94	3.58	3.30	3.46	3.81	2.66	4.65	3.99	3.82	4.85
	dt_gbm	1.96	12.00	10.15	11.37	10.63	7.18	3.63	4.52	2.91	1.78	1.93	2.29	1.47	2.26	0.00
	dt_rf	4.06	12.10	8.95	10.75	10.13	8.25	5.38	2.46	2.63	1.25	1.46	1.37	1.91	0.00	1.38
higgs	lpm_gbm	29.29	17.80	11.40	6.56	3.06	2.68	3.16	2.90	2.67	2.82	2.65	1.79	2.62	2.19	1.63
	lpm_rf	26.71	17.29	15.06	10.60	5.35	4.04	2.35	2.03	1.66	1.89	2.91	2.94	3.31	2.58	2.22
	dt_gbm	0.00	0.00	1.86	0.26	0.93	0.45	-	-	-	-	-	-	-	-	-
	dt_rf	4.04	1.26	1.74	1.32	1.54	0.91	-	-	-	-	-	-	-	-	-
covtype.binary	lpm_gbm	76.52	66.39	29.17	12.51	9.18	5.28	4.94	4.56	3.92	3.56	3.62	3.31	2.59	2.83	2.39
	lpm_rf	96.77	63.38	14.36	9.61	6.79	3.94	2.93	2.81	2.96	2.84	2.31	2.26	2.00	2.43	2.22
	dt_gbm	0.00	0.00	2.35	1.27	1.18	1.11	0.00	0.00	0.00	-	-	-	-	-	-
	dt_rf	0.00	0.00	2.10	2.33	2.44	2.39	1.84	2.19	1.65	0.70	-	0.89	-	-	-
phishing	lpm_gbm	0.00	1.88	2.88	3.05	3.22	3.25	2.99	1.69	1.42	1.45	1.29	0.00	0.00	0.00	0.00
	lpm_rf	0.00	2.14	3.29	3.22	3.59	3.79	3.29	2.05	1.42	1.44	1.24	1.23	1.16	1.26	1.02
	dt_gbm	0.00	0.00	0.00	0.07	0.39	0.00	0.28	0.22	0.44	0.23	0.00	0.00	0.00	0.00	0.00
	dt_rf	0.00	0.72	0.00	0.57	0.00	<u>-0.17</u>	0.13	0.48	0.13	0.05	0.03	<u>-0.03</u>	<u>-0.28</u>	0.00	<u>-0.16</u>
ala	lpm_gbm	0.00	2.55	7.58	8.98	8.40	8.03	8.90	8.23	8.17	7.90	5.96	7.10	6.97	6.18	5.73
	lpm_rf	0.00	4.17	8.81	9.92	9.88	9.47	8.99	9.31	9.19	9.26	9.33	8.25	7.15	7.55	7.98
	dt_gbm	0.00	5.54	2.39	3.84	3.55	2.55	1.51	2.25	4.87	-	-	-	-	-	-
	dt_rf	0.00	6.44	3.36	5.60	3.40	5.94	6.06	4.97	4.89	4.01	4.73	5.21	-	-	4.53
pendigits	lpm_gbm	51.39	23.44	16.18	8.95	8.84	6.63	4.86	1.83	2.27	2.16	2.44	2.16	3.33	2.97	2.73
	lpm_rf	46.28	22.74	21.72	8.80	8.47	6.29	6.48	1.69	3.03	2.79	2.34	2.68	2.70	3.02	0.00
	dt_gbm	14.02	6.72	5.11	13.14	6.42	4.20	2.46	1.09	0.98	0.16	<u>-0.26</u>	0.00	0.00	0.00	0.00
	dt_rf	21.46	4.18	5.22	14.51	7.36	4.55	2.86	0.00	0.00	0.00	0.00	0.00	0.00	0.00	0.00
letter	lpm_gbm	57.06	48.48	59.85	29.76	36.09	19.27	20.37	16.08	17.55	15.16	17.26	16.51	18.46	17.19	15.55
	lpm_rf	61.06	65.34	64.26	23.69	35.20	26.15	22.10	20.74	20.91	20.31	19.28	21.40	20.77	19.39	18.18
	dt_gbm	0.00	13.98	25.05	33.96	32.05	15.49	11.17	0.00	4.26	3.50	1.99	0.00	0.00	0.00	0.00
	dt_rf	0.00	12.21	28.67	33.47	33.51	18.41	8.10	0.00	1.84	1.21	1.31	0.67	0.61	0.11	<u>-0.08</u>
Sensorless	lpm_gbm	216.47	257.56	178.31	117.01	90.70	83.90	73.50	65.95	61.57	57.97	56.54	57.15	55.45	66.24	68.24
	lpm_rf	224.18	210.28	134.44	115.00	85.85	74.96	66.77	61.10	66.88	64.65	69.00	70.09	72.91	80.14	82.15
	dt_gbm	<u>-0.01</u>	42.42	68.13	44.38	17.39	10.32	1.82	1.44	0.79	0.64	0.41	0.12	0.00	<u>-0.02</u>	0.34
	dt_rf	0.00	52.54	57.10	44.61	16.63	6.19	2.19	0.96	0.51	0.00	0.48	0.33	0.00	0.00	0.10
senseit.aco	lpm_gbm	173.71	170.68	63.95	44.20	33.49	22.99	19.14	13.50	10.29	7.59	6.26	5.92	5.30	4.89	4.32
	lpm_rf	177.67	181.26	79.86	42.86	37.60	28.80	23.75	19.06	13.91	10.74	8.48	6.09	5.20	5.32	4.62
	dt_gbm	14.89	0.00	3.71	2.32	4.85	0.81	0.00	-	-	-	-	-	-	-	-
	dt_rf	20.03	2.54	3.64	5.91	3.34	2.63	0.00	0.00	-	-	-	-	-	-	-
senseit.sei	lpm_gbm	160.59	65.27	23.44	10.48	6.76	4.86	4.82	4.46	4.79	4.12	4.54	5.17	3.91	4.21	4.46
	lpm_rf	165.98	63.72	31.58	14.94	9.07	5.79	4.95	5.07	5.24	4.70	4.60	3.74	4.30	4.35	4.35
	dt_gbm	2.66	1.01	3.49	2.29	0.95	1.30	1.37	0.00	-	-	-	-	-	-	-
	dt_rf	2.33	0.00	3.36	1.65	0.87	0.00	<u>-1.23</u>	-	-	-	-	-	-	-	-
covtype	lpm_gbm	36.87	49.24	12.78	11.21	7.84	7.15	7.15	8.07	7.70	8.25	10.94	8.35	4.37	8.77	5.84
	lpm_rf	32.15	39.49	10.49	8.53	8.11	8.59	9.61	11.99	11.22	9.91	8.47	8.16	10.34	13.76	12.92
	dt_gbm	342.27	92.85	43.23	20.04	8.14	8.05	5.67	3.26	4.92	3.52	2.72	0.00	0.00	0.00	1.74
	dt_rf	354.45	98.94	50.87	14.10	9.46	7.38	4.76	4.20	0.94	1.81	2.30	0.71	<u>-0.37</u>	0.00	0.00
connect-4	lpm_gbm	37.62	11.66	12.01	6.84	5.68	6.82	4.58	2.10	3.82	3.21	3.02	3.64	2.32	2.97	3.40
	lpm_rf	33.77	12.99	17.60	14.66	15.91	10.73	6.38	5.35	7.07	6.98	2.84	3.14	2.09	2.52	2.46
	dt_gbm	89.33	29.23	20.20	12.10	9.73	9.88	7.82	7.43	0.57	4.61	1.08	3.35	2.23	1.15	1.55
	dt_rf	113.71	21.91	20.52	11.23	16.86	10.96	10.64	9.11	6.51	5.88	6.76	2.16	2.97	0.61	0.00

A.10 Different Feature Spaces

In our validation experiments in §4.1, the feature vector representation was identical for the oracle and the interpretable model. This is also what Algorithm 1 implicitly assumes.

Here, we consider the possibility of going a step further and using different feature vectors. If f_O and f_I are the feature vector creation functions for the oracle and the interpretable model respectively, and x_i is a “raw data” instance, then:

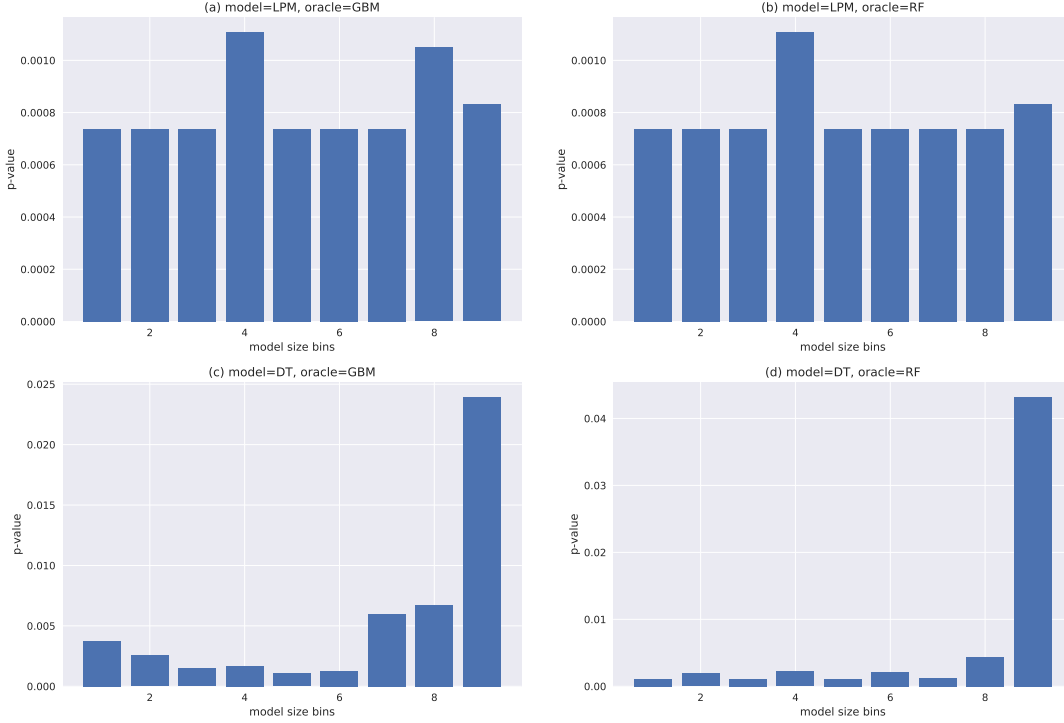


Figure 7: These plots show the p -values for the Wilcoxon signed-rank test, with the null hypothesis H_0 : using the oracle does *not* produce better F1 test scores. The bin boundaries are selected using the *Sturges* rule (Sturges 1926). Low p -values favor our algorithm.

1. The oracle is trained on instances $f_{\mathcal{O}}(x_i)$, and provides uncertainties $u_{\mathcal{O}}(f_{\mathcal{O}}(x_i))$.
2. The interpretable model is provided with data $f_{\mathcal{I}}(x_i)$, but the uncertainty scores available to it are $u_{\mathcal{O}}(f_{\mathcal{O}}(x_i))$.

The motivation for using different feature spaces is that the combination $(\mathcal{O}, f_{\mathcal{O}})$ may be known to work well together and/or a pre-trained oracle might be available only for this combination.

We illustrate this application with the example of predicting nationalities from surnames of individuals. Our dataset (Rao and McMahan 2019) contains examples from 18 nationalities: *Arabic, Chinese, Czech, Dutch, English, French, German, Greek, Irish, Italian, Japanese, Korean, Polish, Portuguese, Russian, Scottish, Spanish, Vietnamese*. The representations and models are as follows:

1. The oracle model is a *Gated Recurrent Unit (GRU)* (Cho et al. 2014), that is learned on the sequence of characters in a surname. The GRU is calibrated with *temperature scaling* (Guo et al. 2017).
2. The interpretable model is a DT, where the features are character n-grams, $n \in 1, 2, 3$. The entire training set is initially scanned to construct an n-gram vocabulary, which is then used to create a sparse binary vector per surname - 1s and 0s indicating the presence and absence of an n-gram respectively.

Figure 9 shows a schematic of the setup.

The n-gram representation leads to a vocabulary of ~ 5000 terms, that is reduced to 600 terms based on a χ^2 -test in the interest of lower running time. DTs of different *depth* ≤ 15 were trained. A budget of $T = 3000$ iterations was used, and the relative improvement in the $F1$ macro score (as in Equation 3) is reported, averaged over three runs. Figure 10 shows the results.

We see large improvements at small depths, that peak with $\delta F1 = 83.04\%$ at *depth* = 3, and then again at slightly larger depths, which peak at *depth* = 9 with $\delta F1 = 12.34\%$.

To obtain a qualitative idea of the changes in the DT using a oracle produces, we look at the prediction rules for *Polish* surnames, when DT *depth* = 3. For each rule, we also present examples of true and false positives.

Baseline rules - *precision* = 2.99%, *recall* = 85.71%, *F1* = 5.77%:

Rule 1. $k \wedge ski \wedge \neg v$

- True Positives: *jaskolski, rudawski*
- False Positives: *skipper (English), babutski (Russian)*

Rule 2. $k \wedge \neg ski \wedge \neg v$

- True Positives: *wawrzaszek, koziol*
- False Positives: *konda (Japanese), jagujinsky (Russian)*

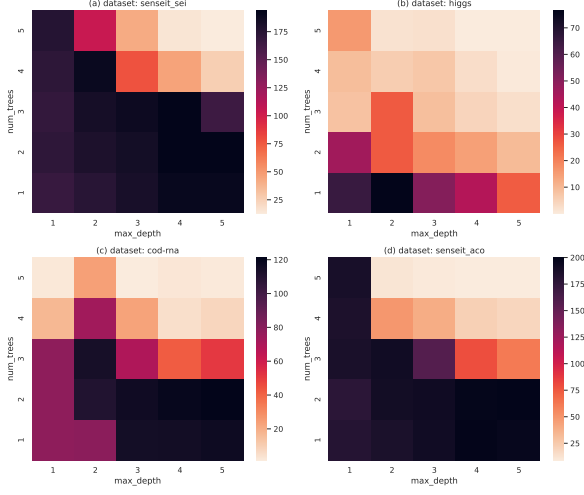


Figure 8: Improvements in test $F1$ -macro for multiple datasets for different sizes of GBM models are shown. (a) Top-left: *senseit-sei* (b) Top-right: *higgs* (c) Bottom-left: *cod-rna* and (d) Bottom-right: *senseit-aco*. Here, model size is the combination of *max_depth* and *number of trees* in the GBM model. Greater improvements are seen at lower sizes.

Oracle-based DT rules - $precision = 25.00\%$, $recall = 21.43\%$, $F1 = 23.08\%$:

Rule 1. $ski \wedge \neg(b \vee kin)$

- True Positives: *jaskolski*, *rudawski*
- False Positives: *skipper* (*English*), *aivazovski* (*Russian*)

We note that the baseline rules are in conflict w.r.t. the literal “ski”, and taken together, they simplify to $k \wedge \neg v$. This makes them extremely permissive, especially *Rule 2*, which requires the literal “k” while needing “ski” and “v” to be absent. Not surprisingly, these rules have high recall ($= 85.71\%$) but poor precision ($= 2.99\%$), leading to $F1 = 5.77\%$.

In the case of the oracle-based DT, now we have only one rule, that requires the atypical trigram “ski”. This improves precision ($= 25\%$), trading off recall ($= 21.43\%$), for a significantly improved $F1 = 23.08\%$.

The difference in rules may also be visualized by comparing the distribution of nationalities represented in their false positives, as in Figure 11. We see that the baseline DT rules, especially *Rule 2*, predict many nationalities, but in the case of the DT learned using the oracle, the model confusion is concentrated around *Russian* names, which is reasonable given the shared *Slavic* origin of many *Polish* and *Russian* names.

We believe this is a particularly powerful and exciting application of our technique, and opens up a wide range of possibilities for translating information between models of varied capabilities.

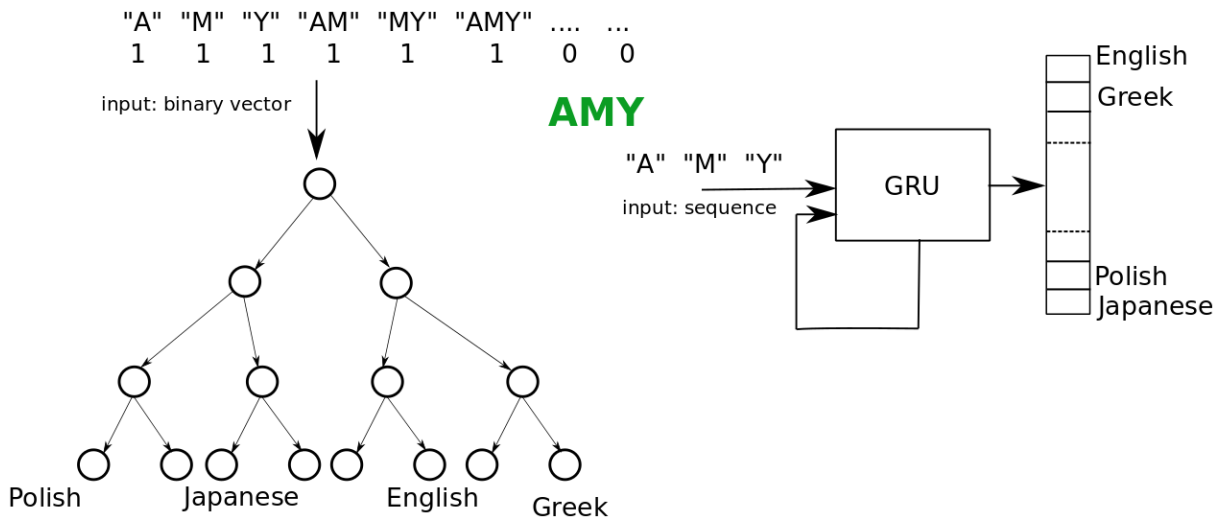


Figure 9: The feature representations for the oracle and the interpretable model may be different. Consider the name “Amy”: the GRU is provided its letters, one at a time, in sequence, while the DT is given an n-gram representation of the name.

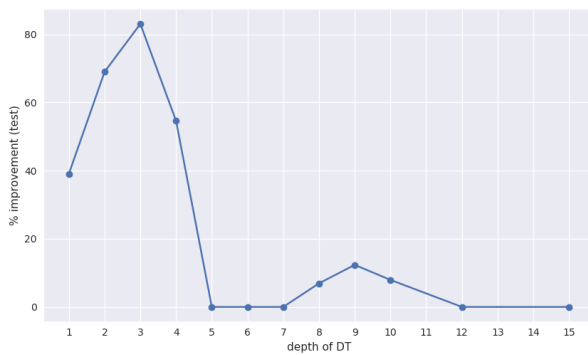


Figure 10: Improvements $\delta F1$ are shown for different depths of the DT. Reproduction of Figure 4, for convenience.

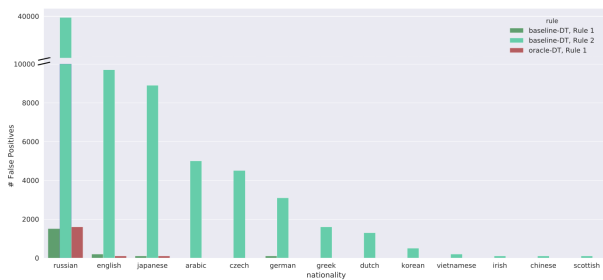


Figure 11: The distribution of nationalities in false positive predictions for the baseline and oracle based models, shown for predicting *Polish* names. Only nationalities with non-zero counts are shown.